

Invited Review, to be published in  
“Recent Research Developments in Astrophysics,”  
by Research Signpost, India 2002

**Complex rotation with internal dissipation.  
Applications to cosmic-dust alignment and to wobbling  
comets and asteroids.**

**Michael Efroimsky**

*Institute for Mathematics and its Applications, University of Minnesota,  
207 Church St. SE, Suite 400, Minneapolis MN 55455, USA*

efroimsk@ima.umn.edu

**Alex Lazarian**

*Departments of Astronomy, University of Wisconsin, 475 North Charter Street,  
Madison WI 53706, USA*

lazarian@astro.wisc.edu

**Vladislav Sidorenko**

*Keldysh Institute of Applied Mathematics, Miusskaja Pl., Dom 4  
Moscow 125047 Russia*

sidorenk@spp.keldysh.ru

## ABSTRACT

Neutron stars, asteroids, comets, cosmic-dust granules, spacecraft, as well as whatever other freely spinning body dissipate energy when they rotate about any axis different from principal. We discuss the internal-dissipation-caused relaxation of a freely precessing rotator towards its minimal-energy mode (mode that corresponds to the spin about the maximal-inertia axis). We show that this simple system contains in itself some quite unexpected physics. While the body nutates at some rate, the internal stresses and strains within the body oscillate at frequencies both higher and (what is especially surprising) lower than this rate. The internal dissipation takes place not so much at the frequency of nutation but rather at the second and higher harmonics. In other words, this mechanical system provides an example of an extreme non-linearity. Issues like chaos and separatrix also come into play. The earlier estimates, that ignored non-linearity, considerably underestimated the efficiency of the internal relaxation of wobbling asteroids and comets. At the same time, owing to the non-linearity of inelastic relaxation, small-angle nutations can persist for very long time spans. The latter circumstance is important for the analysis and interpretation of NEAR’s data on Eros’ rotation state. Regarding the comets, estimates show that the currently available angular resolution of spacecraft-based instruments makes it possible to observe wobble damping within year- or maybe even month-long spans of time. Our review also covers pertinent topics from the cosmic-dust astrophysics; in particular, the role played by precession damping in the dust alignment. We show that this damping provides coupling of the grain’s rotational and vibrational degrees of freedom; this entails occasional flipping of dust grains due to thermal fluctuations. During such a flip, grain preserves its angular momentum, but the direction of torques arising from  $H_2$  formation reverses. As a result, flipping grain will not rotate fast in spite of the action of uncompensated  $H_2$  formation torques. The grains get “thermally trapped,” and their alignment is marginal. Inelastic relaxation competes with the nuclear and Barnett relaxations, so we define the range of sizes for which the inelastic relaxation dominates.

*Subject headings:*

Euler equations, elliptic functions of Jacobi, celestial mechanics, inelastic relaxation, inelastic dissipation, nonlinear dynamics, interstellar medium (ISM), cosmic dust, comets, asteroids, Eros.

PACS: 96.50.Gn, 96.30.Ys, 96.35.Cp, 96.35.Fs, 05.45.-a, 45.40.-f,  
95.10.Ce, 95.10.Fh, 45.50.Pk, 98.38.Cp, 98.58.Ca

## 1. INTRODUCTION

### 1.1. Motivation

On the 14-th of February 1967 the Soviet Union launched artificial spacecraft Kosmos 142, to carry out some ionospheric research. The sputnik had the shape of a cross constituted by four 15-meter-long rods. A separate container, shaped as a cylinder with hemispheres on its ends, was attached in elastic manner to the cross, in a position orthogonal to its plane. This block had dimensions of about  $1.6\text{ m} \times 0.8\text{ m}$ , and carried in itself all the scientific equipment. It was connected to the cross frame by a joint, and it turned out that this perpendicular position of the container was not secured with a sufficient strength. The mission planners wanted the satellite to rotate in the plane of the cross at a rate of 2 revolutions per second. At a certain point, when the spacecraft was yet gaining rotation, deformation started. The cylindrical container overpowered the locking device in the joint, and bent towards the plane of the cross-shaped frame. This phenomenon was addressed by Vasil’ev & Kovtunenکو (1969) who pointed out that the intensity of the effect depends, among other things, upon the angular velocity of rotation of the cross frame. In 22 months after that event, on the 14-th of December 1968, a similar sputnik, Kosmos 259, was launched. Its rotation rate was not so swift: less than one revolution per second. This time no deformations of the spacecraft was observed, and the mission succeeded.

The misadventure of Kosmos 142 resulted from the first principles of mechanics: a freely rotating top must end up in the spin state that minimises the kinetic rotational energy, for a fixed angular momentum. This spin mode can be achieved by one or both of the following means: adjustment of shape or/and alteration of the rotation axis. Since the Russian spacecraft was easily deformable, it “preferred” the first option. Things would go differently if the satellite’s construction were more rigid. The latter effect was observed back in 1958, when the team operating the first American artificial satellite was surprised by some unexpected manoeuvres that the spacecraft suddenly began to carry out. The satellite, called Explorer I, was a very elongated body with four flexible antennas on it. After launching and getting to the orbit, it was set to perform steady rotation about its longest dimension. However, the flight operators never managed to keep the spacecraft in the designed spin state: Explorer persistently deviated from the simple rotation and went into a wobble, exhibiting slowly changing complex spin. Naturally, the rotation state was evolving toward that of minimal kinetic energy (the angular momentum being fixed). We would remind that the state of rotation about the maximal-inertia axis is the one minimising the kinetic energy, while spin about the least-inertia axis corresponds to the maximal energy. Hence, one should expect that the body will (through some dissipative processes) get rid of the excessive energy and will change the spin axis.

Another example of unsupported rotator subject to internal dissipation is a cosmic-dust granule. Due to various spin-up mechanisms (the main of which is catalytic formation of  $H_2$  molecules on the granule surface (Purcell 1979)), these particles spend most part of their

life in rotation. This circumstance gives birth to a whole sequence of subtle effects, which determine alignment of the dust relative to the interstellar magnetic field. This alignment can be indirectly observed through measuring the polarisation degree of the starlight passing through the dust cloud (Lazarian 2000, 1994). It turns out that theoretical description of alignment is based on one’s knowledge of the granules’ typical rotation state: it is important whether the dust particles are, predominantly, in their principal spin states or not (Lazarian & Efrimsky 1999; Efrimsky 2002).

Similar to spacecraft and interstellar grains, a comet or an asteroid in a non-principal rotation mode will dissipate energy and will, accordingly, return to the stable spin (Prendergast 1958, Burns & Safronov 1973, Efrimsky & Lazarian 1999). Nevertheless, several objects were recently found in excited states of rotation. These are asteroid 4179 Toutatis (Ostro et al. 1993, Harris 1994, Ostro et al. 1995, Hudson and Ostro 1995, Scheeres et al. 1998, Ostro et al. 1999) and comet P/Halley (Jewitt 1997; Peale & Lissauer 1989; Sagdeev et al. 1989; Peale 1991; Wilhelm 1987). Quite possibly, tumbling are also comet 46P/Wirtanen (Samarasinha, Mueller & Belton 1996; Rickman & Jorda 1998), comet 29P/Schwachmann-Wachmann 1 (Meech et al 1993). The existing observational data on asteroid 1620 Geographos may, too, be interpreted in favour of wobble (Prokof’eva et al. 1997; Prokof’eva et al. 1996; Ryabova 2002).

The dynamics of a freely rotating body is determined, on the one hand, by the initial conditions of the object’s formation and by the external factors forcing the body out of its principal spin state. On the other hand, it is influenced by the internal dissipation of the excessive kinetic energy associated with wobble. Two mechanisms of internal dissipation are known. The so-called Barnett dissipation, caused by the periodic remagnetisation, is relevant only in the case of cosmic-dust-granule alignment (Lazarian & Draine 1997). The other mechanism, called inelastic relaxation, is, too, relevant for mesoscopic grains, and plays a primary role in the case of macroscopic bodies. Inelastic relaxation results from alternating stresses generated inside a wobbling body by the transversal and centripetal acceleration of its parts. The stresses deform the body, and inelastic effects cause energy dissipation.

The external factors capable of driving a rotator into an excited state are impacts and tidal interactions, the latter being of a special relevance for planet-crossers. In the case of comets, wobble is largely impelled by jetting. Even gradual outgassing may contribute to the effect because a spinning body will start tumbling if it changes its principal axes through a partial loss or redistribution thereof. Sometimes the entire asteroid or comet may be a wobbling fragment of a progenitor disrupted by a collision (Asphaug & Scheeres 1999, Giblin & Farinella 1997, Giblin et al. 1998) or by tidal forces. All these factors, that excite rotators, compete with the inelastic dissipation that always tends to return the rotator to the minimal-energy state.

Study of comets’ and asteroids’ rotation states may provide much information about their recent history and internal structure. However, theoretical interpretation of the observational data will become possible only after we understand quantitatively how inelastic dissipation

affects rotation. The kinetic energy of rotation will decrease at a rate equal to that of energy losses in the material. Thus, one should first calculate the elastic energy stored in a tumbling body, and then calculate the energy-dissipation rate, using the material quality factor  $Q$ . This empirical factor is introduced for a phenomenological description of the overall effect of the various attenuation mechanisms (Nowick & Berry 1972; Burns 1986, 1977; Knopoff 1963; Goldreich & Soter 1965). A comprehensive discussion of the  $Q$ -factor of asteroids and of its frequency- and temperature-dependence is presented in Efroimsky & Lazarian (2000).

## 1.2. Complex Rotation of a Rigid Body

Our review addresses unsupported rotation of rigid and not-entirely-rigid objects. Stated differently, we intend to describe behaviour of unsupported rotators of two sorts: ideal (i.e., those that are exempt from internal dissipation) and realistic (i.e., those subject to dissipation). While the role of dissipative phenomena in the rotating top has become an issue only less than half a century ago, complex rotation of an ideal (absolutely rigid) top has been on the scientific agenda since, at least, the mid of XVIII-th century. This problem generated some of the major mathematical advances carried out by Jacobi, Poinsot and other eminent scholars. However, the founding father of this line of study was Euler whose first notes on the topic date back to 1750's.

Leonhard Euler, the most prolific scientist of all times, will forever retain an aura of mystery in the eyes of historians. Very few researchers, if any, shared his power of insight and his almost superhuman working ability. His life in science consisted of three major periods: the first Russian period (which began in 1730, when young Euler retired from the Russian navy for the sake of academic career), the Berlin period (that started in 1741, when Euler assumed a high administrative position at the Berlin Academy), and the second Russian period (which began in 1765, when major disagreements with King Frederick the Second moved Euler to accept an invitation from Empress Catherine the Great, to return to St.Petersburg). Each of these three periods in Euler's life was marked by numerous scientific achievements in all areas of mathematics known at that epoch.

One of the fields, that grossly benefitted from Euler's attention during his tenure in Berlin, was mechanics of an unsupported top. Euler wrote ca 1760 his pivotal result on the topic (Euler 1765), his famous equations:

$$\frac{d}{dt}(I_i \Omega_i) - (I_j - I_k) \Omega_j \Omega_k = \tau_i \quad , \quad (1-1)$$

where  $I_{1,2,3}$  are the eigenvalues of inertia tensor of the body. The tensor is defined through

$$I_{ij} \equiv \int dm \{ \vec{\rho}^2 \delta_{ij} - \rho_i \rho_j \} \quad , \quad (1-2)$$

$\vec{\rho}$  being the position of mass element  $dm$  relative to the centre of mass of the body. Equations (1-1) are merely a reformulation of the simple fact that the torque equals the rate

of change of the angular momentum. They express this law in **a** body frame. Among the body frames, there exists one (called principal) wherein the inertia tensor is diagonal. In (1-1),  $\Omega_{1,2,3}$  are the angular-velocity components as measured in that, principal, coordinate system. Quantities  $\tau_i$  are principal-axes-related components of the total torque acting on the body. As ever, we shall assume without loss of generality that  $I_3 \geq I_2 \geq I_1$ . Hence the third axis will always be that of major inertia.

In the body frame, the period of angular-velocity precession about the principal axis 3 is:  $\tau = 2\pi/\omega$ . Evidently,

$$\dot{\Omega}_i/\Omega_i \approx \tau^{-1} \quad , \quad \dot{I}_i/I_i \approx \tau^{-1} \epsilon \quad , \quad (1-3)$$

$\epsilon$  being a typical value of the relative strain that is several orders less than unity. These estimates lead to the inequality  $\dot{I}_i \Omega_i \ll I_i \dot{\Omega}_i$ , thereby justifying the commonly used approximation to Euler's equations<sup>1</sup>:

$$I_i \dot{\Omega}_i - (I_j - I_k) \Omega_j \Omega_k = \tau_i \quad . \quad (1-4)$$

Naturally, this elegant system of equations has carried since its birth the name of its author. It took scientists some more years to understand that the system deserves its given name for one more reason: formulae (1.1) are exactly the Euler-Lagrange equations for the Lagrangian of an unsupported rigid body. Proof of this fact demands a certain effort. A brief (but still not trivial) derivation offered in 1901 by Poincare can be found in the textbook by Marsden (2000).

The Euler equations simplify considerably when two of three moments of inertia  $I_i$  are equal. This is called dynamic symmetry, to distinguish it from the full geometric symmetry. Further on, whenever we refer to symmetric top, we shall imply only the dynamic symmetry, not the geometric one. This case was addressed by Euler (1765) himself, and later by Lagrange (1813) and Poisson (1813). For prolate symmetric rotators (i.e., when  $I_3 = I_2 > I_1$ ), in the absence of external torques, the solution is simple:

$$\Omega_1 = \text{const} \quad , \quad \Omega_2 = \Omega_{\perp} \sin \omega t \quad , \quad \Omega_3 = \Omega_{\perp} \cos \omega t \quad , \quad (1-5)$$

where  $\omega = (I_1/I_3 - 1)\Omega_1$ . We see that, from the viewpoint of an observer placed on the rotating body, the vector of inertial angular velocity  $\vec{\Omega}$  describes a circular cone about the minor-inertia axis (1) of the body. So does the angular-momentum vector  $\vec{J}$ . Both  $\vec{\Omega}$  and

---

<sup>1</sup> Rigorously speaking, in the case when the approximation (1-3) is not satisfied, not only (1-4) fail but even equations (1-1) must be somewhat amended. The problem arises from the ambiguity in the choice of the body frame. For example, if we prefer to choose the coordinate system wherein the inertia tensor always remains diagonal, then the angular momentum will be different from zero in the body frame (and will be of order  $\epsilon$ ). If, though, we choose the coordinates in which the angular momentum vanishes, then the inertia matrix will no longer be diagonal. With this choice of the body frame, (1-1) should rather be written down not in terms of  $I_i$  but in terms of all  $I_{ij}$ . We shall not elaborate on this issue in our review.

$\vec{\mathbf{J}}$  precess about the least-inertia axis at the same rate  $\omega = (I_1/I_3 - 1)\Omega_1$ , though at different angles from the axis.

In an inertial coordinate system, the angular momentum  $\vec{\mathbf{J}}$  will not precess, because it must keep constant for a free rotator. Instead, it is the least-inertia axis (1) and the angular velocity  $\vec{\Omega}$  that precess about  $\vec{\mathbf{J}}$ , in an inertial observer's opinion. (For brevity, we denote each vector by one letter, though we, of course, imply that every vector transforms appropriately whenever the coordinate system is changed.)

In the case of oblate (dynamic) symmetry (  $I_3 > I_2 = I_1$  ) free precession will be expressed, in the body frame, by solution

$$\Omega_1 = \Omega_{\perp} \cos \omega t \quad , \quad \Omega_2 = \Omega_{\perp} \sin \omega t \quad , \quad \Omega_3 = \text{const} \quad (1-6)$$

where  $\omega = (I_3/I_1 - 1)\Omega_3$  is the mutual rate of circular precession of  $\vec{\Omega}$  and  $\vec{\mathbf{J}}$  about the major inertia axis (3).

The general case of  $I_3 > I_2 \geq I_1$  is quite involved and demands numerics (see Mitchell & Richardson (2001); Richardson & Mitchell (1999), and references therein). Still, in the absence of external torques the problem can be solved analytically, and Euler coped with it (Euler 1765), though to that end he had to introduce functions similar to what we now call elliptic integrals. The solution much simplifies when expressed through the elliptic functions of Jacobi  $sn$ ,  $cn$ ,  $dn$ . These were defined and studied by Karl Jacobi (1829) and used by him (Jacobi 1849, 1882) to describe free rotation. Jacobi's functions are generalisations of the trigonometric ones, in the following sense: while for symmetric prolate and oblate rotators the circular precession is expressed by (1-5) and (1-6) correspondingly, in the general case  $I_3 \geq I_2 \geq I_1$  precession is expressed by very similar formulae that contain Jacobi's functions instead of sin and cos :

$$\Omega_1 = \gamma \, dn(\omega t, k^2) \quad , \quad \Omega_2 = \beta \, sn(\omega t, k^2) \quad , \quad \Omega_3 = \alpha \, cn(\omega t, k^2) \quad , \quad (1-7)$$

for  $\mathbf{J}^2 < 2 I_2 T_{kin}$  , and

$$\Omega_1 = \tilde{\gamma} \, cn(\tilde{\omega} t, \tilde{k}^2) \quad , \quad \Omega_2 = \tilde{\beta} \, sn(\tilde{\omega} t, \tilde{k}^2) \quad , \quad \Omega_3 = \alpha \, dn(\tilde{\omega} t, \tilde{k}^2) \quad (1-8)$$

for  $\mathbf{J}^2 > 2 I_2 T_{kin}$  . Here the precession rate  $\omega$  and the parameters  $\alpha$ ,  $\beta$ ,  $\tilde{\beta}$ ,  $\gamma$ ,  $\tilde{\gamma}$ ,  $\tilde{\omega}$ ,  $k$  and  $\tilde{k}$  are certain combinations of  $I_{1,2,3}$ ,  $T_{kin}$  and  $\mathbf{J}^2$  . We see that (1-7) is a generalisation of (1-5), while (1-8) is that of (1-6). Solution (1-7) approaches (1-5) in the limit of prolate symmetry,  $(I_3 - I_2)/I_1 \rightarrow 0$  , while solution (1-8) approaches (1-6) in the limit of oblate symmetry,  $(I_2 - I_1)/I_1 \rightarrow 0$  . This situation is illustrated by Figure 1. To understand this picture, one should keep in mind that two quantities are conserved for a freely-spinning body: the angular momentum

$$\vec{\mathbf{J}}^2 = I_1^2 \Omega_1^2 + I_2^2 \Omega_2^2 + I_3^2 \Omega_3^2 \quad , \quad (1-9)$$

(which is conserved exactly) and the kinetic energy

$$T_{kin} = \frac{1}{2} \{ I_1 \Omega_1^2 + I_2 \Omega_2^2 + I_3 \Omega_3^2 \} \quad . \quad (1-10)$$

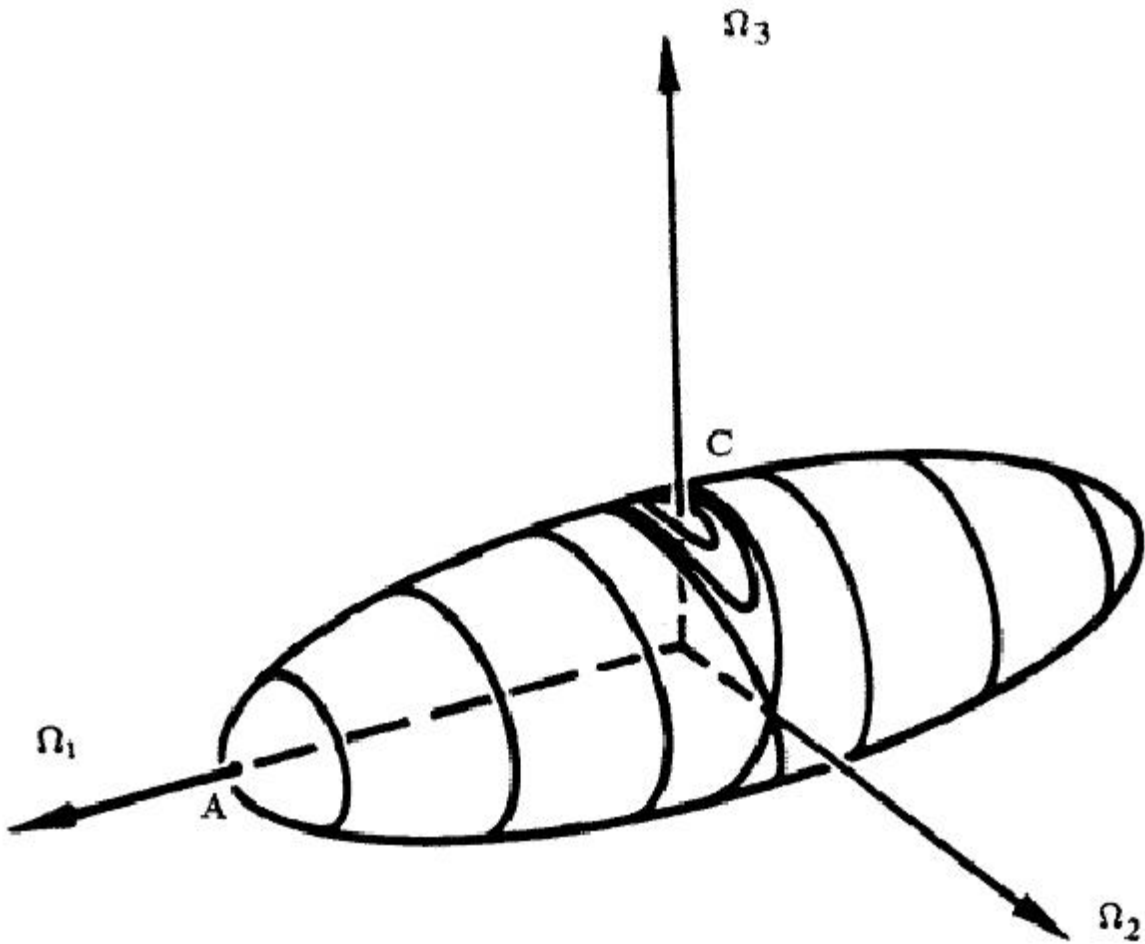


Fig. 1.— The constant-angular-momentum ellipsoid, in the angular-velocity space. The lines on its surface are its intersections with the kinetic-energy ellipsoids corresponding to different values of the rotational energy. The quasi-stable pole A is the maximal-energy configuration, i.e., the state wherein the body spins about its minimal-inertia axis. The stable pole C symbolises the minimal-energy state, i.e., rotation about the maximal-inertia axis. The angular-velocity vector describes the constant-energy lines, and at the same time slowly shifts from one line to another, approaching pole C. The picture illustrates the case of an elongated body:  $I_3 \gtrsim I_2 > I_1$ . The trajectories are circular near A and remain (in the case of an elongated body) virtually circular almost up to the separatrix. The trajectories will regain a circular shape only in the closest proximity of C.



(which is conserved only approximately because of the internal dissipation). Expressions (1-9) and (1-10) define ellipsoids in the angular-velocity space  $(\Omega_1, \Omega_2, \Omega_3)$ . Intersection of these gives the trajectory described by the tip of vector  $\vec{\Omega}$  in the angular-velocity space. On the picture we see the angular-momentum ellipsoid (1-9) with lines marked on its surface. These lines are its intersection with ellipsoids (1-10) appropriate to several different values of energy  $T_{kin}$ . For a fixed value of  $\vec{J}^2$ , i.e., for a fixed angular-momentum surface (1-9), there exists an infinite family of kinetic-energy surfaces (1-10) intersecting with it. The largest surface of kinetic energy (corresponding to the maximal value of  $T_{kin}$ ) will be an ellipsoid that fully encloses our angular-momentum ellipsoid and only touches it in point A and its opposite. Similarly, the smallest surface of kinetic energy (corresponding to minimal  $T_{kin}$ ) will be an ellipsoid escribed by our angular-momentum ellipsoid and only touching it from inside, at point C and its opposite. For a fixed  $\vec{J}$ , the maximal and minimal possible values of the kinetic energy are achieved during rotations about the minimal-inertia and maximal-inertia axes, appropriately. In the case of a non-dissipative torque-free rotation, the tip of vector  $\vec{\Omega}$  will be describing, on Fig. 1, a curve along which the angular-momentum and energy ellipsoids intersect (Lamy & Burns 1972). Solution (1-7) is valid for higher energies, i.e., from point A through the separatrix. In astronomy such rotations are called LAM (= Long-Axis Modes). Solution (1-8) works for lower energies, i.e., from the separatrix through point C. Such rotations are called SAM (= Short-Axis Modes). Wherever the trajectories on Fig.1, i.e, in the space  $(\Omega_1, \Omega_2, \Omega_3)$ , are almost circular<sup>2</sup>, the solutions (1-7) and (1-8) may be approximated by (1-5) and (1-6), correspondingly. In the limit of an oblate rotator, the applicability domain of (1-7) will shrink into a point (or, to be more exact, into two points: A and its opposite). Similarly, in the limit of a prolate body, the applicability region of (1-8) will shrink into two points: C and its opposite.

### 1.3. Realistic Rotators

The formalism developed by Euler and refined by Jacobi might be a perfect tool for description of rotation of asteroids, comets, cosmic-dust granules, spacecraft and whatever other unsupported rigid rotators, if not for one circumstance, inner dissipation. Because of this circumstance, the Euler-Jacobi theory of precession works only for time spans short enough to neglect kinetic-energy losses.

The necessity of internal dissipation follows from the basic principles of mechanics. A freely spinning body of a fixed angular momentum has kinetic energy whose values are constrained to lie within a certain bounded range. Hence, from the physical viewpoint, it is very natural for this body to be seeking ways of relaxation. In other words, the body must “do its best” to get rid of the excessive kinetic energy, in order to approach the minimal-energy

---

<sup>2</sup>Be mindful that the trajectory in the space  $(\Omega_1, \Omega_2, \Omega_3)$  being almost circular does not necessarily mean that the precession cone of the major-inertia axis about  $\vec{J}$  is circular or almost circular.

configuration. Thence the necessity of some dissipation mechanism.

Two such mechanisms are known. One is relevant only for mesoscopic rotators, like interstellar-dust grains, and therefore plays a certain role in the cosmic-dust alignment. This is the Barnett dissipation, a phenomenon called into being by periodic remagnetisation of a precessing paramagnetic body (Lazarian & Draine 1997).

The second mechanism, inelastic dissipation, is, too, relevant for mesoscopic grains (Lazarian & Efroimsky 1999), and it plays the decisive role in the macroscopic bodies' relaxation. The effect results from the alternating stresses produced inside a wobbling body by the time-dependent acceleration of its parts. The stresses deform the body, and the inelastic effects cause dissipation of the rotational energy.

Dissipation entails relaxation of the precession: the major-inertia axis of the body and its angular-velocity vector  $\vec{\Omega}$  tend to align along the angular momentum  $\vec{J}$ . In other words, the precession cone described by  $\vec{\Omega}$  about  $\vec{J}$  will be narrowing until  $\vec{\Omega}$  aligns along  $\vec{J}$  completely. A simple calculation (Efroimsky 2001, Efroimsky 2000, Efroimsky & Lazarian 2000, Lazarian & Efroimsky 1999) shows that in this case the major-inertia axis of the body will align in the same direction, so that, from the body-frame viewpoint,  $\vec{\Omega}$  will eventually be pointing along this axis. This configuration will correspond to the minimal kinetic energy, the angular momentum being fixed.

An inertial observer will thus see the unsupported body miraculously changing its rotation axis. This is exactly what happened in 1958 when, to mission experts' surprise, rotating satellite Explorer I changed its rotation axis and went into wobble (Thomson 1961).

This was, probably, the first example of a practical need for a further development of the Eulerian theory of a free top, a development that would address an unsupported top with dissipation. However, Chandrasekhar realised this already in mid-50s, after having been alerted by Kuiper, and asked a postdoc, Kevin Prendergast, to look into that<sup>3</sup>. The most general question was (and still is): how many asteroids in the Solar System can be in non-principal (i.e., nutating) spin states, and how can this evidence of the impact frequency in the main belt? Prendergast in his paper (1958) implied that it is collisions<sup>4</sup> that drive asteroids out of the principal state and make them wobble. An important point made by Prendergast (1958) was generation of the second harmonic in a symmetrical oblate rotator: if a body is precessing at an angular rate  $\omega$ , then the dissipation is taking place not only at this frequency but also at double thereof. Prendergast considered only the deceptively simple case of symmetrical rotator, and therefore failed to notice the emergence of harmonics higher than the second. Besides, the mathematical treatment of the problem, offered in his paper, was erroneous in several other aspects. Nevertheless, the fact that he noticed the second

---

<sup>3</sup> The authors are grateful to Tom Gehrels for providing these historical facts.

<sup>4</sup> The collisions within the main belt became a popular topic much later, in 90-s. See, for example, (dell'Oro, Paolicchi, Cellino, Zappala, Tanga, & Michel 2001).

harmonic was by itself an important contribution for which Prendergast should be credited. His paper was published much ahead of time and, therefore, was forgotten. Independently from Prendergast, Lazarian and Efroimsky (1999) came across the second harmonic some 40 years later. Generation of the higher harmonics was pointed out only in (Efroimsky 2000). The reason why the important work by Prendergast was not fully appreciated by his contemporaries is that back in 50-s the observational astronomy lacked any reliable data on wobbling asteroids. So, Prendergast’s paper went almost unnoticed, and his successors had to start up from scratch.

The interest in the asteroidal precession re-emerged in 70-s, after the publication of the milestone work by Burns & Safronov (1973) that suggested estimates for the relaxation time, based on the decomposition of the deformation pattern into bulge flexing and bending, and also on the conjecture that “the centrifugal bulge and its associated strains wobble back and forth relative to the body as the rotation axis  $\omega$  moves through the body during a wobble period.” As turned out later, the latter conjecture was a too strong statement, because the inelastic dissipation, for the most part of it, is taking place not near the surface but in the depth of the body, i.e., not right under the bulge but deep beneath it. Thus, the bulge is much like an iceberg tip. This became clear when the distribution of precession-caused stresses was calculated, with improved boundary conditions (Efroimsky & Lazarian 2000), (Lazarian & Efroimsky 1999)<sup>5</sup>. Burns & Safronov’s treatment neglected the nonlinearity, i.e., generation of frequencies higher and lower than the nutation rate. The nonlinearity, in fact, is essential. Its neglect leads to a large underestimation of the damping rate, because in many spin states a considerable input comes from the harmonics (Efroimsky & Lazarian 2000), (Efroimsky 2000). The neglect of nonlinearity leads to up to a two-order underestimate of the precession-damping rate.

In the same year, Peale published an article dealing with inelastic relaxation of nearly spherical bodies (Peale 1973), and there he did take the second harmonic into account.

In 1979 Purcell addressed a similar problem of interstellar-grain precession damping. He ignored the harmonics and mishandled the boundary conditions upon stresses: in (Purcell 1979) the normal stresses had their maximal values on the free surfaces and vanished in the centre of the body (instead of being maximal in the centre and vanishing on the surfaces). These oversights lead to a several-order underevaluation of the dissipation effectiveness and, thereby, of the relaxation rate.

---

<sup>5</sup> This topic will be discussed in section 4. Our treatment of stresses, demonstrated there, is not mathematically rigorous either. It is a polynomial approximation which satisfies the boundary conditions only approximately. From the physical viewpoint, it is not worth further refining that treatment, because the slight mishandling of the boundary conditions “spoils” the solution much less than the irregularity and inhomogeneity of a the realistic body.

### 1.4. Precession damping

The dynamics of precession relaxation is described by the angular rate of alignment of the maximal-inertia axis (3) along the angular momentum  $\vec{J}$ , i.e., by the decrease in angle  $\theta$  between these. In the case of oblate symmetry (when  $I_3 > I_2 = I_1$ ), this angle remains adiabatically unchanged over the precession period, which makes  $d\theta/dt$  a perfect measure of the damping rate (Efroimsky & Lazarian 2000). However, in the general case of a triaxial body angle  $\theta$  evolves periodically through the precession cycle. To be more exact, it evolves *almost* periodically, and its value at the end of the cycle is only slightly different from that in the beginning of the cycle. The relaxation is taking place through accumulation of these slight variations over many periods. This is called adiabatic regime, i.e., regime with two different time scales: we have a “fast” process (precession) and a “slow” process (relaxation). Under the adiabaticity assumption, one may average  $\theta$ , or some function thereof, over the precession cycle. Then the damping rate will be described by the evolution of this average. Technically, it is convenient to use the average of its squared sine (Efroimsky 2000). One can write for a triaxial rotator:

$$\frac{d \langle \sin^2 \theta \rangle}{dt} = \frac{d \langle \sin^2 \theta \rangle}{dT_{kin}} \frac{dT_{kin}}{dt} , \quad (1-11)$$

while for an oblate one the expression will look simpler:

$$\left( \frac{d\theta}{dt} \right)_{(oblate)} = \left( \frac{d\theta}{dT_{kin}} \right)_{(oblate)} \frac{dT_{kin}}{dt} . \quad (1-12)$$

The derivatives  $d \langle \sin^2 \theta \rangle / dT_{kin}$  and  $(d\theta/dT_{kin})_{(oblate)}$  appearing in (1-11) and (1-12) indicate how the rotational-energy dissipation affects the value of  $\langle \sin^2 \theta \rangle$  (or simply of  $\theta$ , in the oblate case). These derivatives can be calculated from the equations of motion (see Efroimsky & Lazarian (2000) and Efroimsky (2000)). The kinetic-energy decrease,  $dT_{kin}/dt$ , is caused by the inelastic dissipation:

$$dT_{kin}/dt = \langle dW/dt \rangle , \quad (1-13)$$

$W$  being the energy of the alternating stresses, and  $\langle \dots \rangle$  denoting an average over a precession cycle. (This averaging is justified within the adiabatic approach. For details see section III below.) Finally, in the general case of a triaxial top, the alignment rate will read:

$$\frac{d \langle \sin^2 \theta \rangle}{dt} = \frac{d \langle \sin^2 \theta \rangle}{dT_{kin}} \frac{d \langle W \rangle}{dt} , \quad (1-14)$$

and for a symmetrical oblate top:

$$\left( \frac{d\theta}{dt} \right)_{(oblate)} = \left( \frac{d\theta}{dT_{kin}} \right)_{(oblate)} \frac{d \langle W \rangle}{dt} . \quad (1-15)$$

Now we are prepared to set out the strategy of our further work. While calculation of  $d \langle \sin^2 \theta \rangle / dT_{kin}$  and  $(d\theta/dT_{kin})_{oblate}$  is an easy exercise<sup>6</sup>, our main goal will be to find the

---

<sup>6</sup>See formula (4-18) below and also formulae (A12 - A13) in Efroimsky 2000.

dissipation rate  $d \langle W \rangle / dt$ . This quantity will consist of inputs from the dissipation rates at all the frequencies involved in the process, i.e., from the harmonics at which stresses oscillate in a body precessing at a given rate  $\omega$ . The stress is a tensorial extension of the notion of a pressure or force. Stresses naturally emerge in a spinning body due to the centripetal and transversal accelerations of its parts. Due to the precession, these stresses contain time-dependent components. If we find a solution to the boundary-value problem for alternating stresses, it will enable us to write down explicitly the time-dependent part of the elastic energy stored in the wobbling body, and to separate contributions from different harmonics:

$$\langle W \rangle = \sum_n \langle W(\omega_n) \rangle \quad . \quad (1-16)$$

$W(\omega_n)$  being the elastic energy of stresses alternating at frequency  $\omega_n$ . One should know each contribution  $W(\omega_n)$ , for these will determine the dissipation rate at the appropriate frequency, through the frequency-dependent empirical quality factors. The knowledge of these factors, along with the averages  $\langle W(\omega_n) \rangle$ , will enable us to find the dissipation rates at each harmonic. Sum of those will give the entire dissipation rate due to the alternating stresses emerging in a precessing body.

### 1.5. Inelastic dissipation caused by complex rotation

Equation (1-16) implements the most important observation upon which all our study rests: generation of harmonics in the stresses inside a precessing rigid body. The harmonics emerge because the acceleration of a point inside a precessin body contains centrifugal terms that are quadratic in the angular velocity  $\vec{\Omega}$ . In the simplest case of a symmetrical oblate body, for example, the body-frame-related components of the angular velocity are given in terms of  $\sin \omega t$  and  $\cos \omega t$  (see formulae (1-5) - (1-6)). Evidently, squaring of  $\vec{\Omega}$  will yield terms both with  $\sin \omega t$  or  $\cos \omega t$  and with  $\sin 2\omega t$  or  $\cos 2\omega t$ . The stresses produced by this acceleration will, too, contain terms with frequency  $\omega t$  as well as those with the harmonic  $2\omega t$ . In the further sections we shall explain that a triaxial body precessing at rate  $\omega$  is subject, in distinction from a symmetrical oblate body, to a superposition of stresses oscillating at frequencies  $\omega_n = n\omega_1$ , the "base frequency"  $\omega_1$  being lower than the precession rate  $\omega$ . The basic idea is that in the general, non-oblate case, the time dependence of the acceleration and stresses will be expressed not by trigonometric but by elliptic functions whose expansions over the trigonometric functions will generate an infinite number of harmonics. In subsection 4.3 we shall explain this in more detail.

The total dissipation rate will be a sum of the particular rates (Stacey 1992) to be calculated empirically. The empirical description of attenuation is based on the quality factor  $Q(\omega)$  and on the assumption of attenuation rates at different harmonics being independent from one another:

$$\dot{W} = \sum_n \dot{W}(\omega_n) = - \sum_n \frac{\omega_n W_0(\omega_n)}{Q(\omega_n)} = - 2 \sum_n \frac{\omega_n \langle W(\omega_n) \rangle}{Q(\omega_n)} \quad (1-17)$$

$Q(\omega)$  being the quality factor of the material, and  $W_0(\omega_n)$  and  $\langle W(\omega_n) \rangle$  being the maximal and the average values of the appropriate-to- $\omega_n$  fraction of elastic energy stored in the body. This expression will become more general if we put the quality factor under the integral, implying its possible coordinate dependence<sup>7</sup>:

$$\dot{W} = -2 \sum_{\omega_n} \int dV \left\{ \frac{\omega_n}{Q(\omega_n)} \frac{d \langle W(\omega_n) \rangle}{dV} \right\} , \quad (1-18)$$

The above assumption of attenuation rates at different harmonics being mutually independent is justified by the extreme smallness of strains (typically, much less than  $10^{-6}$ ) and by the frequencies being extremely low ( $10^{-5} - 10^{-3} \text{ Hz}$ ). One, thus, may say that the problem is highly nonlinear, in that we shall take into account the higher harmonics in the expression for stresses. At the same time, the problem remains linear in the sense that we shall neglect any nonlinearity stemming from the material properties (in other words, we shall assume that the strains are linear function of stresses). We would emphasize, though, that the nonlinearity is most essential, i.e., that the harmonics  $\omega_n$  come to life unavoidably: no matter what the properties of the material are, the harmonics do emerge in the expressions for stresses. Moreover, as we shall see, the harmonics interfere with one another due to  $W$  being quadratic in stresses. Generally, all the infinite amount of multiples of  $\omega_1$  will emerge. The oblate case, where only  $\omega_1$  and  $2\omega_1$  show themselves, is an exception. Another exception is the narrow-cone precession of a triaxial rotator studied in Efroimsky (2000): in the narrow-cone case, only the first and second modes are relevant (and  $\omega_1 \approx \omega$ ).

Often the overall dissipation rate, and therefore the relaxation rate is determined mostly by harmonics rather than by the principal frequency. This fact was discovered only recently (Efroimsky & Lazarian 2000, Efroimsky 2000, Lazarian & Efroimsky 1999), and it led to a considerable re-evaluation of the effectiveness of the inelastic-dissipation mechanism. In some of the preceding publications, its effectiveness had been underestimated by several orders of magnitude, and the main reason for this underestimation was neglect of the second and higher harmonics. As for the choice of values of the quality factor  $Q$ , Prendergast (1958) and Burns & Safronov (1973) borrowed the terrestrial seismological data for  $Q$ . In Efroimsky & Lazarian (2000), we argue that these data may be inapplicable to asteroids.

To calculate the afore mentioned average energies  $\langle W(\omega_n) \rangle$ , we use such entities as stress and strain. As already mentioned above, the stress is a tensorial generalisation of the notion of pressure. The strain tensor is analogous to the stretching of a spring (rendered in dimensionless fashion by relating the displacement to the base length). Each tensor component of the stress consists of two inputs, elastic and plastic. The former is related to the strain through the elasticity constants of the material; the latter is related to the time-derivative of the strain, through the viscosity coefficients. As our analysis is aimed at extremely small deformations of cold bodies, the viscosity may well be neglected, and the stress tensor will be approximated, to a high accuracy, by its elastic part. Thence, according to Landau &

---

<sup>7</sup>In strongly inhomogeneous nutating bodies attenuation may depend on location.

Lifshitz (1976), the components of the elastic stress tensor  $\sigma_{ij}$  are interconnected with those of the strain tensor  $\epsilon_{ij}$  like:

$$\epsilon_{ij} = \delta_{ij} \frac{Tr \sigma}{9 K} + \left( \sigma_{ij} - \frac{1}{3} \delta_{ij} Tr \sigma \right) \frac{1}{2 \mu} \quad , \quad (1-19)$$

$\mu$  and  $K$  being the *adiabatic* shear and bulk moduli, and  $Tr$  standing for the trace of a tensor.

To simplify the derivation of the stress tensor, the body will be modelled by a rectangular prism of dimensions  $2a \times 2b \times 2c$  where  $a \geq b \geq c$ . The tensor is symmetrical and is defined by

$$\partial_i \sigma_{ij} = \rho a_j \quad , \quad (1-20)$$

$a_j$  being the time-dependent parts of the acceleration components, and  $\rho a_j$  being the time-dependent parts of the components of the force acting on a unit volume<sup>8</sup>. Besides, the tensor  $\sigma_{ij}$  must obey the boundary conditions: its product by normal unit vector,  $\sigma_{ij} n_j$ , must vanish on the boundaries of the body (this condition was not fulfilled in Purcell (1979)).

Solution to the boundary-value problem provides such a distribution of the stresses and strains over the body volume that an overwhelming share of dissipation is taking place not near the surface but in the depth of the body. For this reason, the prism model gives a good approximation to realistic bodies. Still, in further studies it will be good to generalise our solution to ellipsoidal shapes. The first step in this direction has been made by Molina, Moreno & Martinez-López (2002).

Equation (1-20) has a simple scalar analogue<sup>9</sup>. Consider a non-rotating homogeneous liquid planet of radius  $R$  and density  $\rho$ . Let  $g(r)$  and  $P(r)$  be the free-fall acceleration and the self-gravitational pressure at the distance  $r \leq R$  from the centre. (Evidently,  $g(r) = (4/3) \pi G \rho r$ .) Then the analogue to (1-20) will read:

$$\rho g(r) = - \frac{\partial P(r)}{\partial r} \quad , \quad (1-21)$$

the expression  $\rho g(r)$  standing for the gravity force acting upon a unit volume, and the boundary condition being  $P(R) = 0$ . Solving equation (1-21) reveals that the pressure has a maximum at the centre of the planet, although the force is greatest at the surface. Evidently, the maximal deformations (strains) also will be experienced by the material near the centre of the planet.

In our case, the acceleration  $\vec{a}$  of a point inside the precessing body will be given not by the free-fall acceleration  $g(\vec{r})$  but will be a sum of the centripetal and transversal accelerations:  $\vec{\Omega} \times (\vec{\Omega} \times \vec{r}) + \dot{\vec{\Omega}} \times \vec{r}$ , the Coriolis term being negligibly small. Thereby,

---

<sup>8</sup>Needless to say, these acceleration components  $a_j$  are not to be mixed with  $a$  which is the longest dimension of the prism.

<sup>9</sup>This example was kindly offered to us by William Newman.

the absolute value of  $\vec{\alpha}$  will be proportional to that of  $\vec{\mathbf{r}}$ , much like in the above example. In distinction from the example, though, the acceleration of a point inside a wobbling top will have both a constant and a periodic component, the latter emerging due to the precession. For example, in the case of a symmetrical oblate rotator, the precessing components of the angular velocity  $\vec{\Omega}$  will be proportional to  $\sin\omega t$  and  $\cos\omega t$ , whence the transversal acceleration will contain frequency  $\omega$  while the centripetal one will contain  $2\omega$ . The stresses obtained through (1-20) will oscillate at the same frequencies, and so will the strains. As we already mentioned, in the case of a non-symmetrical top an infinite amount of harmonics will emerge, though these will be overtones not of the precession rate  $\omega$  but of some different "base frequency"  $\omega_1$  that is less than  $\omega$ .

Here follows the expression for the (averaged over a precession period) elastic energy stored in a unit volume of the body:

$$\frac{d \langle W \rangle}{dV} = \frac{1}{2} \langle \epsilon_{ij} \sigma_{ij} \rangle = \frac{1}{4\mu} \left\{ \left( \frac{2\mu}{9K} - \frac{1}{3} \right) \langle (Tr \sigma)^2 \rangle + \langle \sigma_{ij} \sigma_{ij} \rangle \right\} =$$

$$\frac{1}{4\mu} \left\{ -\frac{1}{1 + \nu^{-1}} \langle (Tr \sigma)^2 \rangle + \langle \sigma_{xx}^2 \rangle + \langle \sigma_{yy}^2 \rangle + \langle \sigma_{zz}^2 \rangle + 2 \langle \sigma_{xy}^2 + \sigma_{yz}^2 + \sigma_{zx}^2 \rangle \right\} \quad (1-22)$$

where  $2\mu/(9K) - 1/3 = -\nu/(1+\nu) \approx -1/5$ ,  $\nu$  being Poisson's ratio (for most solids  $\nu \approx 1/4$ ). Naturally<sup>10</sup>, the total averaged elastic energy is given by the integral over the body's volume:

$$\langle W \rangle = \frac{1}{2} \int dV \sigma_{ij} \epsilon_{ij} \quad , \quad (1-23)$$

and it must be expanded into the sum (1-16) of inputs from oscillations of stresses at different frequencies. Each term  $\langle W(\omega_n) \rangle$  emerging in that sum will then be plugged into the expression (1-17), together with the value of  $Q$  appropriate to the overtone  $\omega_n$ .

## 2. NONLINEARITY, CHAOS, SEPARATRIX

### 2.1. The Origin of the Nonlinearity

When (1-18) is inserted into (1-14) and (1-15), one can explicitly see the contributions to the entire effect, coming from the principal frequency  $\omega_1$  and from the harmonics  $\omega_n \equiv n\omega_1$ . When vector  $\vec{\Omega}$  describes approximately circular trajectories on Figure 1, the principal frequency  $\omega_1$  virtually coincides with the precession rate  $\omega$ . This doesn't hold, though, when  $\vec{\Omega}$  get closer to the separatrix: there  $\omega_1$  becomes *lower* than the precession rate. The analysis of the stress and strain distributions, and the resulting expressions for  $d \langle W \rangle / dt$  written down in (Efroimsky & Lazarian 2000) and (Efroimsky 2000) shows that the nonlinearity is

---

<sup>10</sup>Very naturally indeed, because, for example,  $\sigma_{xx}\epsilon_{xx}dV = (\sigma_{xx} dy dz)(\epsilon_{xx} dx)$  is a product of the  $x$ -directed pressure upon the  $x$ -directed elongation of the elementary volume  $dV$ .



essential, in that the generation of harmonics is not a high-order effect but a phenomenon playing a key role in the relaxation process. In other words, dissipation associated with the harmonics is often of the same order as that at the principal frequency. Near the separatrix it may be even higher.

The nonlinearity emerges due to the simple fact that the acceleration of a point within a wobbling object contains centrifugal terms that are quadratic in the angular velocity  $\vec{\Omega}$ . In neglect of small terms caused by the body deformation, the acceleration will read:

$$\vec{\mathbf{a}} = \dot{\vec{\Omega}} \times \vec{\mathbf{r}} + \vec{\Omega} \times (\vec{\Omega} \times \vec{\mathbf{r}}) \quad . \quad (2-1)$$

$\mathbf{a}$  being the acceleration in the inertial frame, and  $\vec{\mathbf{r}}$  being the position of a point. In the simplest case of oblate symmetry, the body-frame-related components of the angular velocity are expressed by (1-5) plugging whereof into (2-1) produces terms containing  $\sin \omega t$  and  $\cos \omega t$ , as well as those containing  $\sin 2\omega t$  and  $\cos 2\omega t$ . The alternating stresses and strains caused by this acceleration are linear functions of  $\mathbf{a}$  and, thus, will also contain the second harmonic, along with the principal frequency. Calculation of the stresses, strains, and of the appropriate elastic energy  $W$  is then only a matter of some elaborate technique. This technique (presented in (Efroimsky & Lazarian 2000) and (Efroimsky 2001)) leads to an expression for  $W$ , with contributions from  $\omega$  and  $2\omega$  explicitly separated. The nonlinearity is essential: in many rotation states the  $2\omega$  input in (1-14), (1-15). is of order and even exceeds that coming from the principal frequency  $\omega$ . To explain in brief the reason why the nonlinearity is strong, we would mention that while the acceleration and the stresses and strains are quadratic in the (precessing) angular velocity  $\vec{\Omega}$ , the elastic energy is proportional to the product of stress and strain tensors. Hence the elastic energy is proportional to the fourth power of  $\vec{\Omega}$ .

## 2.2. The Near-Separatrix Slowing-Down of the Precession (Lingering Effect)

In the general case of a triaxial rotator, precession is described by (1-7) or (1-8). The acceleration of a point inside the body (and, therefore, the stresses and strains in the material) will, according to (2-1), contain terms quadratic in the Jacobi functions. These functions can be decomposed in converging series (the so-called nome expansions) over  $\sin$ 'es and  $\cos$ 'ines of  $n\nu$ ,  $n$  being odd integers for  $sn(\omega t, k^2)$  and  $cn(\omega t, k^2)$  and even integers for  $dn(\omega t, k^2)$ . Here  $\nu$  is a frequency *lower* than the precession rate  $\omega$ :

$$\nu = \omega \frac{2\pi}{4K(k^2)} \quad , \quad (2-2)$$

$4K(k^2)$  being the mutual period of  $sn$  and  $cn$ . Near the poles  $\nu \rightarrow \omega$ , while on approach to the separatrix  $\nu \rightarrow 0$ . When two such expansions get multiplied by one another, they produce a series containing all sorts of products like  $(\sin m\nu t \sin n\nu t)$ ,  $(\cos m\nu t \cos n\nu t)$ ,

and cross terms. Hence the acceleration, stress and strain contain the entire multitude of overtones. Even though the further averaging of  $W$  over the precession cycle weeds out much of these terms, we are eventually left with all the harmonics on our hands.

As explained in (Efroimsky 2000), higher-than-second harmonics will bring only high-order contributions to the precession-relaxation process when the rotation state is described by a point close to poles A or C. Put differently, it is sufficient to take into account only the frequencies  $\nu \approx \omega$  and  $2\nu \approx 2\omega$ , insofar as the trajectories on Figure 1 are approximately circular (i.e., when (1-6) and (1-7) are well approximated by (1-2) and (1-5)). Near the separatrix the situation is drastically different, in that all the harmonics become important. We thus transit from the domain of essential nonlinearity into the regime of extreme nonlinearity, regime where the higher harmonics bring more in the process than  $\nu$  or  $2\nu$ . We are reminded, however, that en route to the separatrix we not just get all the multiples of the principal frequency, but we face a change of the principal frequency itself: according to (2-2), the principal frequency  $\nu$  will be lower than the precession rate  $\omega$ ! This regime may be called “exotic nonlinearity”.

Without getting bogged down in involved mathematics (to be attended to in subsection 4.3 below), we would just mention here that in the limit of  $\vec{\Omega}$  approaching the separatrix the dissipation rate will vanish, in the adiabatic approximation. This may be guessed even from the fact that in the said limit  $\nu \rightarrow 0$ . We thus come to an important conclusion that the relaxation rate, being very high at a distance from the separatrix, decreases in its closest vicinity. Can we, though, trust that the relaxation rate completely vanishes on the separatrix? No, because in the limit of  $\vec{\Omega}$  approaching the separatrix the adiabatic approximation will fail. In other words, it will not be legitimate to average the energy dissipation over the precession cycle, because near the separatrix the precession rate will not necessarily be faster than the relaxation rate. A direct calculation shows that even on the separatrix itself the acceleration of a point within the body will remain finite (but will, of course, vanish at the unstable middle-inertia pole). The same can be said about stress, strain and the relaxation rate. So what we eventually get is not a near-separatrix trap but just lingering: one should expect relaxing tops to considerably linger near the separatrix. As for Explorer, it is now understandable why it easily went wobbling but did not rush to the minimal-energy spin state: it couldn’t cross the separatrix so quickly. We would call it “lingering effect”. There is nothing mysterious in it. The capability of near-intermediate-axis spin states to mimic simple rotation was pointed out by Samarasingha, Mueller & Belton (1999) with regard to comet Hale-Bopp. A similar setting was considered by Chernous’ko (1968) who studied free precession of a tank filled with viscous liquid and proved that in that case the separatrix is crossed within a finite time interval<sup>11</sup>.

---

<sup>11</sup>Such problems have been long known also to mathematicians studying the motion with a non-Hamiltonian perturbation: the perturbation wants the system to cross the separatrix, but is not guaranteed to succeed in it, because some trajectories converge towards the unstable pole (Neishtadt 1980)

### 3. THE APPLICABILITY REALM OF THE ADIABATIC APPROACH

In the beginning of subsection 1.2 we explained that Euler’s equations (1-1) may be written down in their approximate form (1-4) in case the nutation-caused deformations of the body are negligibly small. Thus it turns out that in our treatment the same phenomenon is neglected in one context and accounted for in another: on the one hand, the very process of the inelastic dissipation stems from the precession-inflicted small deformations; on the other hand, we neglect these deformations in order to write down (1-4). This approximation (also discussed in Lambeck 1988) may be called adiabatic, and it remains acceptable insofar as the relaxation is slow against rotation and precession. To cast the adiabatic approximation into its exact form, one should first come up with a measure of the relaxation rate. Clearly, this should be the time derivative of the angle  $\theta$  made by the major-inertia axis  $\mathbf{3}$  and the angular momentum  $\mathbf{\bar{J}}$ . The axis aligns towards  $\mathbf{\bar{J}}$ , so  $\theta$  must eventually decrease. Be mindful, though, that even in the absence of dissipation,  $\theta$  does evolve in time, as can be shown from the equations of motion. Fortunately, this evolution is periodic, so one may deal with a time derivative of the angle averaged over the precession period. In practice, it turns out to be more convenient to deal with the squared sine of  $\theta$  (Efroimsky 2000) and to write the adiabaticity assertion as:

$$-\frac{d\langle \sin^2 \theta \rangle}{dt} \ll \omega , \tag{3-1}$$

$\omega$  being the precession rate and  $\langle \dots \rangle$  being the average over the precession period. The case of an oblate symmetrical top<sup>12</sup> is exceptional, in that  $\theta$  remains, when dissipation is neglected, constant over a precession cycle. No averaging is needed, and the adiabaticity condition simplifies to:

$$-\left(\frac{d\theta}{dt}\right)_{(oblate)} \ll \omega . \tag{3-2}$$

We would emphasise once again that the distinction between the oblate and triaxial cases, distinction resulting in the different forms of the adiabaticity condition, stems from the difference in the evolution of  $\theta$  in the weak-dissipation limit. The equations of motion of an oblate rotator show that, in the said limit,  $\theta$  stays virtually unchanged through a precession cycle (see section IV below). So the slow decrease of  $\theta$ , accumulated over many periods, becomes an adequate measure for the relaxation rate. The rate remains slow, compared to the rotation and precession, insofar as (3-2) holds. In the general case of a triaxial top the equations of motion show that, even in the absence of dissipation, angle  $\theta$  periodically evolves, though its average over a cycle stays unchanged (virtually unchanged, when dissipation is present but weak)<sup>13</sup>. In this case we should measure the relaxation rate by the accumulated, over many cycles, change in the average of  $\theta$  (or of  $\sin^2 \theta$ ). Then our assumption about the relaxation being slow yields (1-15)

<sup>12</sup>Hereafter oblate symmetry will imply not a geometrical symmetry but only the so-called dynamical symmetry:  $I_1 = I_2$ .

<sup>13</sup>See formulae (A1) - (A4) in the Appendix to Efroimsky 2000.

The above conditions (3-1) - (3-2) foreshadow the applicability domain of our further analysis. For example, of the two quantities,

$$I_1^2 \Omega_1^2 + I_2^2 \Omega_2^2 + I_3^2 \Omega_3^2 = \vec{\mathbf{J}}^2 \quad , \quad (3-3)$$

$$I_1 \Omega_1^2 + I_2 \Omega_2^2 + I_3 \Omega_3^2 = 2 T_{kin} \quad , \quad (3-4)$$

only the former will conserve exactly, while the latter will remain virtually unchanged through one cycle and will be gradually changing through many cycles (just like  $\langle \sin^2 \theta \rangle$  ).

## 4. SYMMETRIC AND ASYMMETRIC ROTATORS

### 4.1. Precession of an Oblate Body.

An oblate body has moments of inertia that relate as:

$$I_3 > I_2 = I_1 \equiv I \quad . \quad (4-1)$$

We shall be interested in  $\dot{\theta}$ , the rate of the maximum-inertia axis' approach to the direction of angular momentum  $\vec{\mathbf{J}}$ . To achieve this goal, we shall have to know the rate of energy losses caused by the periodic deformation. To calculate this deformation, it will be necessary to find the acceleration experienced by a particle located inside the body at a point  $(x, y, z)$ . Note that we address the inertial acceleration, i.e., the one with respect to the inertial frame  $(X, Y, Z)$ , but we express it in terms of coordinates  $x, y$  and  $z$  of the body frame  $(1, 2, 3)$  because eventually we shall have to compute the elastic energy stored in the entire body (through integration of the elastic-energy density over the body volume).

The fast motions (revolution and precession) obey, in the adiabatical approximation, the simplified Euler equations (1-14). Their solution, with neglect of the slow relaxation, looks (Fowles and Cassiday 1986, Landau and Lifshitz 1976), in the oblate case (4-1):

$$\Omega_1 = \Omega_{\perp} \cos \omega t \quad , \quad \Omega_2 = \Omega_{\perp} \sin \omega t \quad , \quad \Omega_3 = const \quad (4-2)$$

where

$$\Omega_{\perp} \equiv \Omega \sin \alpha \quad , \quad \Omega_3 \equiv \Omega \cos \alpha \quad , \quad (4-3)$$

$\alpha$  being the angle made by the major-inertia axis 3 with  $\vec{\mathbf{\Omega}}$ . Expressions (4-2) show that in the body frame the angular velocity  $\vec{\mathbf{\Omega}}$  describes a circular cone about the principal axis 3 at a constant rate

$$\omega = (h - 1)\Omega_3, \quad h \equiv I_3/I \quad . \quad (4-4)$$

So angle  $\alpha$  remains virtually unchanged through a cycle (though in the presence of dissipation it still may change gradually over many cycles). The precession rate  $\omega$  is of the same order as  $|\vec{\mathbf{\Omega}}|$ , except in the case of  $h \rightarrow 1$  or in a very special case of  $\vec{\mathbf{\Omega}}$  and  $\vec{\mathbf{J}}$  being orthogonal or almost orthogonal to the maximal-inertia axis 3. Hence one may call not only

the rotation but also the precession “fast motions” (implying that the relaxation process is a slow one). Now, let  $\theta$  be the angle between the principal axis 3 and the angular-momentum  $\vec{\mathbf{J}}$ , so that  $J_3 = J \cos \theta$  and

$$\Omega_3 \equiv \frac{J_3}{I_3} = \frac{J}{I_3} \cos \theta \quad (4-5)$$

wherefrom

$$\omega = (h - 1) \frac{J}{I_3} \cos \theta \quad . \quad (4-6)$$

Since, for an oblate object,

$$\vec{\mathbf{J}} = I_1 \Omega_1 \mathbf{e}_1 + I_2 \Omega_2 \mathbf{e}_2 + I_3 \Omega_3 \mathbf{e}_3 = I (\Omega_1 \mathbf{e}_1 + \Omega_2 \mathbf{e}_2) + I_3 \Omega_3 \mathbf{e}_3 \quad , \quad (4-7)$$

the quantity  $\Omega_\perp \equiv \sqrt{\Omega_1^2 + \Omega_2^2}$  is connected with the absolute value of  $\mathbf{J}$  like:

$$\Omega_\perp = \frac{J}{I} \sin \theta = \frac{J}{I_3} h \sin \theta \quad , \quad h \equiv I_3/I \quad . \quad (4-8)$$

It ensues from (4-3) that  $\Omega_\perp/\Omega_3 = \tan \alpha$ . On the other hand, (4-5) and (4-8) entail:  $\Omega_\perp/\Omega_3 = h \tan \theta$ . Hence,

$$\tan \alpha = h \tan \theta \quad . \quad (4-9)$$

We see that angle  $\theta$  is almost constant too (though it gradually changes through many cycles). We also see from (4-7) that in the body frame the angular-momentum vector  $\mathbf{J}$  describes a circular cone about axis 3 with the same rate  $\omega$  as  $\Omega$ . An inertial observer, though, will insist that it is rather axis 3, as well as the angular velocity  $\Omega$ , that is describing circular cones around  $\vec{\mathbf{J}}$ . It follows trivially from (4-4) and (4-7) that

$$I \vec{\boldsymbol{\Omega}} = \vec{\mathbf{J}} - I \omega \vec{\mathbf{e}}_3 \quad , \quad (4-10)$$

whence it is obvious that, in the inertial frame, both  $\vec{\boldsymbol{\Omega}}$  and axis 3 are precessing about  $\vec{\mathbf{J}}$  at rate  $J/I$ . (The angular velocity of this precession is  $\dot{\vec{\mathbf{e}}}_3 = \vec{\boldsymbol{\Omega}} \times \vec{\mathbf{e}}_3 = (\vec{\mathbf{J}}/I - \omega \vec{\mathbf{e}}_3) \times \vec{\mathbf{e}}_3 = (\mathbf{J}/I) \times \vec{\mathbf{e}}_3$ .) Interestingly, the rate  $\omega = (h - 1) \Omega_3$ , at which  $\vec{\boldsymbol{\Omega}}$  and  $\vec{\mathbf{J}}$  are precessing about axis 3 in the body frame, differs considerably from the rate  $J/I$  at which  $\vec{\boldsymbol{\Omega}}$  and axis 3 are precessing around  $\vec{\mathbf{J}}$  in the inertial frame. (In the case of the Earth,  $J/I \approx 400\omega$  because  $h$  is close to unity.) Remarkably, the inertial-frame-related precession rate is energy-independent and, thus, stays unchanged through the relaxation process. This is not the case for the body-frame-related rate  $\omega$  which, according to (4-6), gradually changes because so does  $\theta$ .

As is explained above, we shall be interested in the body-frame-related components  $\Omega_{1,2,3}$  precessing at rate  $\omega$  about the principal axis 3. Acceleration of an arbitrary point of the body can be expressed in terms of these components through formula

$$\vec{\mathbf{a}} = \vec{\mathbf{a}}' + \dot{\vec{\boldsymbol{\Omega}}} \times \vec{\mathbf{r}}' + 2 \vec{\boldsymbol{\Omega}} \times \vec{\mathbf{v}}' + \vec{\boldsymbol{\Omega}} \times (\vec{\boldsymbol{\Omega}} \times \vec{\mathbf{r}}') \quad , \quad (4-11)$$

where  $\vec{\mathbf{r}}$ ,  $\vec{\mathbf{v}}$ ,  $\vec{\mathbf{a}}$  are the position, velocity and acceleration in the inertial frame, and  $\vec{\mathbf{r}}'$ ,  $\vec{\mathbf{v}}'$  and  $\vec{\mathbf{a}}'$  are those in the body frame. Here  $\vec{\mathbf{r}} = \vec{\mathbf{r}}'$ . Mind though that  $\vec{\mathbf{v}}'$  and  $\vec{\mathbf{a}}'$  do not vanish in the body frame. They may be neglected on the same grounds as term  $\dot{I}_i \Omega_i$  in (1-11): precession of a body of dimensions  $\sim l$ , with period  $\tau$ , leads to deformation-inflicted velocities  $v' \approx \epsilon l/\tau$  and accelerations  $a' \approx \epsilon l/\tau^2$ ,  $\epsilon$  being the typical order of strains arising in the material. Clearly, for very small  $\epsilon$ , quantities  $v'$  and  $a'$  are much less than the velocities and accelerations of the body as a whole (that are about  $l/\tau$  and  $l/\tau^2$ , correspondingly). Neglecting these, we get, from (4-11) and (4-2), for the acceleration at point  $(x, y, z)$ :

$$\begin{aligned} \vec{\mathbf{a}} = & \vec{\mathbf{e}}_1 \left\{ \frac{1}{2} \Omega_{\perp}^2 x \cos 2\omega t + \frac{1}{2} \Omega_{\perp}^2 y \sin 2\omega t + z \Omega_{\perp} \Omega_3 h \cos \omega t \right\} + \\ & + \vec{\mathbf{e}}_2 \left\{ \frac{1}{2} \Omega_{\perp}^2 x \sin 2\omega t - \frac{1}{2} \Omega_{\perp}^2 y \cos 2\omega t + z \Omega_{\perp} \Omega_3 h \sin \omega t \right\} + \\ & + \vec{\mathbf{e}}_3 \left\{ \Omega_{\perp} \Omega_3 (2 - h) (x \cos \omega t + y \sin \omega t) \right\} . \end{aligned} \quad (4-12)$$

Substitution thereof into (1-20), with the proper boundary conditions imposed, yields, for an oblate prism of dimensions  $2a \times 2a \times 2c$ ,  $a > c$ , to the following **approximate** expressions:

$$\sigma_{xx} = \frac{\rho \Omega_{\perp}^2}{4} (x^2 - a^2) \cos 2\omega t , \quad \sigma_{yy} = -\frac{\rho \Omega_{\perp}^2}{4} (y^2 - a^2) \cos 2\omega t , \quad \sigma_{zz} = 0 \quad (4-13)$$

$$\sigma_{xy} = \frac{\rho}{4} \Omega_{\perp}^2 (x^2 + y^2 - 2a^2) \sin 2\omega t , \quad (4-14)$$

$$\sigma_{xz} = \frac{\rho}{2} \Omega_{\perp} \Omega_3 [ h (z^2 - c^2) + (2 - h) (x^2 - a^2) ] \cos \omega t , \quad (4-15)$$

$$\sigma_{yz} = \frac{\rho}{2} \Omega_{\perp} \Omega_3 [ h (z^2 - c^2) + (2 - h) (y^2 - a^2) ] \sin \omega t . \quad (4-16)$$

In (4-12) - (4-16) we kept only time-dependent parts, because time-independent parts of the acceleration, stresses and strains are irrelevant in the context of dissipation. A detailed derivation of (4-12) - (4-16) is presented in (Lazarian & Efroimsky 1999).

Formulae (4-13) - (4-16) implement the polynomial approximation to the stress tensor. This approximation keeps the symmetry and obeys (1-20) with (4-12) plugged into it. The boundary condition are satisfied exactly for the diagonal components and only approximately for the off-diagonal components. The approximation considerably simplifies calculations and entails only minor errors in the numerical factors in (4-22).

The second overtone emerges, along with the principal frequency  $\omega$ , in the expressions for stresses since the centripetal part of the acceleration is quadratic in  $\Omega$ . The kinetic energy of an oblate spinning body reads, according to (1-10), (4-3), and (4-9):

$$T_{kin} = \frac{1}{2} [ I \Omega_{\perp}^2 + I_3 \Omega_3^2 ] = \frac{1}{2} \left[ \frac{1}{I} \sin^2 \theta + \frac{1}{I_3} \cos^2 \theta \right] J^2 , \quad (4-17)$$

wherefrom

$$\frac{dT_{kin}}{d\theta} = \frac{J^2}{I_3} (h - 1) \sin \theta \cos \theta = \omega J \sin \theta . \quad (4-18)$$

The latter expression, together with (1-15) and (1-22), leads to:

$$\frac{d\theta}{dt} = \left( \frac{dT_{kin}}{d\theta} \right)^{-1} \frac{dT_{kin}}{dt} = (\omega J \sin \theta)^{-1} \dot{W} , \quad (4-19)$$

where

$$\dot{W} = \dot{W}^{(\omega)} + \dot{W}^{(2\omega)} = -\omega \frac{W_0^{(\omega)}}{Q^{(\omega)}} - 2\omega \frac{W_0^{(2\omega)}}{Q^{(2\omega)}} \approx \quad (4-20)$$

$$\approx -\frac{2\omega}{Q} \{ \langle W^{(\omega)} \rangle + 2 \langle W^{(2\omega)} \rangle \} , \quad (4-21)$$

the quality factor assumed to depend upon the frequency very weakly<sup>14</sup>. In the above formula,  $W_0^\omega$  and  $W_0^{2\omega}$  are amplitudes of elastic energies corresponding to the principal mode and the second harmonic. Quantities  $\langle W^\omega \rangle = W_0^\omega/2$  and  $\langle W^{2\omega} \rangle = W_0^{2\omega}/2$  are the appropriate averages. Substitution of (4-13) - (4-16) into (1-22), with further integration over the volume and plugging the result into (1-15), will give us the final expression for the alignment rate:

$$d\theta/dt = -\frac{3}{2^4} \sin^3 \theta \frac{63 (c/a)^4 \cot^2 \theta + 20}{[1 + (c/a)^2]^4} \frac{a^2 \Omega_0^3 \rho}{\mu Q} \quad (4-22)$$

where

$$\Omega_0 \equiv \frac{J}{I_3} \quad (4-23)$$

is a typical angular velocity. Deriving (4-22), we took into account that, for an oblate  $2a \times 2a \times 2c$  prism (where  $a > c$ ), the moment of inertia  $I_3$  and the parameter  $h$  read:

$$I_3 = \frac{16}{3} \rho a^4 c \quad , \quad h \equiv \frac{I_3}{I} = \frac{2}{1 + (c/a)^2} . \quad (4-24)$$

Details of derivation of (4-22) are presented in (Lazarian & Efroimsky 1999)<sup>15</sup>.

Formula (4-22) shows that the major-inertia axis slows down its alignment at small residual angles. For  $\theta \rightarrow 0$ , the derivative  $\dot{\theta}$  becomes proportional to  $\theta$ , and thus,  $\theta$  decreases exponentially slowly:  $\theta = A \exp(-\zeta t)$ , where  $A$  and  $\zeta$  are some positive numbers<sup>16</sup>. This

<sup>14</sup>The  $\omega$ -dependence of  $Q$  should be taken into account within frequency spans of several orders, but is irrelevant for frequencies differing by a factor of two.

<sup>15</sup>Our expression (4-22) presented here differs from the appropriate formula in Lazarian & Efroimsky (1999) by a factor of 2, because in Lazarian & Efroimsky (1999) we missed the coefficient 2 connecting  $W_0^{(\dots)}$  with  $W^{(\dots)}$ .

<sup>16</sup>This resembles the behaviour of a pendulum: if the pendulum is initially given exactly the amount of kinetic energy sufficient for the pendulum to move up and to point upwards at the end of its motion, then formally it takes an infinite time for the pendulum to stand on end.

feature, "exponentially slow finish", (which was also mentioned, with regard to the Chandler wobble, in Peale (1973), formula (55)) is natural for a relaxation process, and does not lead to an infinite relaxation time if one takes into account the finite resolution of the equipment. Below we shall discuss this topic at length.

Another feature one might expect of (4-22) would be a "slow start": it would be good if  $d\theta/dt$  could vanish for  $\theta \rightarrow \pi/2$ . If this were so, it would mean that at  $\theta = \pi/2$  (i.e., when the major-inertia axis is exactly perpendicular to the angular-momentum vector) the body "hesitates" whether to start aligning its maximal-inertia axis along or opposite to the angular momentum, and the preferred direction is eventually determined by some stochastic influence from the outside, like (say) a collision with a small meteorite. This behaviour is the simplest example of the famous spontaneous symmetry breaking, and in this setting it is desirable simply for symmetry reasons:  $\theta = \pi/2$  must be a position of an unstable equilibrium<sup>17</sup>. Contrary to these expectations, though, (4-22) leaves  $d\theta/dt$  nonvanishing for  $\theta \rightarrow \pi/2$ , bringing an illusion that the major axis leaves the position  $\theta = \pi/2$  at a finite rate. This failure of our formula (4-22) comes from the inapplicability of our analysis in the closest vicinity of  $\theta = \pi/2$ . This vicinity simply falls out of the adiabaticity domain of our treatment, because  $\omega$  given by (4-6) vanishes for  $\theta \rightarrow \pi/2$  (then one can no longer assume the relaxation to be much slower than the precession rate, and hence, the averaging over period becomes illegitimate). This is explained in more detail in the next subsection.

One more situation, that does not fall under the auspices of our analysis, is when  $\omega$  vanishes due to  $(h - 1) \rightarrow 0$ . This happens when  $c/a$  approaches unity. According to (4-22), it will appear that  $d\theta/dt$  remains nonvanishing for  $c/a \rightarrow 1$ , though on physical grounds the alignment rate must decay to zero because, for  $c = a$ , the body simply lacks a major-inertia axis.

All in all, (4-22) works when  $\theta$  is not too close to  $\pi/2$  and  $c/a$  is not too close to unity:

$$-\dot{\theta} \ll (h - 1) \frac{J}{I_3} \cos \theta = \frac{1 - (c/a)^2}{1 + (c/a)^2} \Omega_0 \cos \theta \quad . \quad (4-25)$$

Knowledge of the alignment rate  $\dot{\theta}$  as a function of the precession-cone half-angle  $\theta$  enables one not only to write down a typical relaxation time but to calculate the entire dynamics of the process. In particular, suppose the observer is capable of measuring the precession-cone half-angle  $\theta$  with an error  $\delta$ . This observer will then compute, by means of (4-22), the time needed for the body to change its residual half-angle from  $\theta$  to  $\theta - \Delta\theta$ , for  $\Delta\theta > \delta$ .

---

<sup>17</sup>Imagine a knife freely rotating about its longest dimension, and let the rotation axis be vertical. This rotation mode is unstable, and the knife must eventually come to rotation about its shortest dimension, the blade being in the horizontal plane. One cannot say, though, which of the two faces of the blade will look upward and which downward. This situation is also illustrated by the pendulum mentioned in the previous footnote: when put upside down on its end, the pendulum "hesitates" in what direction to start falling, and the choice of direction will be dictated by some infinitesimally weak exterior interaction (like a sound, or trembling of the pivot, or an evanescent flow of air).



This time will then be compared with the results of his further measurements. Below we shall show that such observations will soon become possible for spacecraft.

## 4.2. Precession of an Exactly Symmetrical Prolate Body.

At the first glance, the dynamics of a freely-spinning elongated body obeys the same principles as that of an oblate one: the axis of maximal inertia will tend to align itself parallel to the angular momentum. If we assume that the body is (dynamically) prolate (i.e., that  $I_3 = I_2 > I_1$ ), it will, once again, be convenient to model it by a prism of dimensions  $2a \times 2a \times 2c$ , though this time half-size  $c$  will be larger than  $a$ . Then all our calculations will *formally* remain in force, up to formula (4-18): since the factor  $h-1 = [1-(c/a)^2]/[1+(c/a)^2]$  is now negative, the right-hand side in (4-18) will change its sign:

$$\frac{dT_{kin}}{d\theta} = \frac{J^2}{I_3} (h - 1) \sin \theta \cos \theta = -\omega J \sin \theta . \quad (4-26)$$

Thereby formula (4-19) will also acquire a “minus” sign in its right-hand side:

$$\frac{d\theta}{dt} = \left( \frac{dT_{kin}}{d\theta} \right)^{-1} \frac{dT_{kin}}{dt} = -(\omega J \sin \theta)^{-1} \dot{W} \quad (4-27)$$

Formula (4-21) will remain unaltered. Eventually, by using (4-27) and (4-21), we shall arrive to a formula that differs from (4-22) only by a sign, provided  $\theta$  still denotes the angle between  $\vec{\mathbf{J}}$  and the body-frame axis 3 (parallel to dimension  $2c$ ):

$$d\theta/dt = \frac{3}{2^4} \sin^3 \theta \frac{63 (c/a)^4 \cot^2 \theta + 20}{[1 + (c/a)^2]^4} \frac{a^2 \Omega_0^3 \rho}{\mu Q} \quad (4-28)$$

This looks as if axis 3 tends to stand orthogonal to  $\vec{\mathbf{J}}$ , which is natural since axis 3 is now not the maximal-inertia but the minimal-inertia axis.

Alas, all this extrapolation is of marginal practical interest, because even a small difference between  $I_2$  and  $I_3$  leads to a considerably different type of rotation. This circumstance was pointed out by Black et al (1999) and was comprehensively discussed by Efroimsky (2000). Without getting into excessive mathematical details, here we shall provide a simple qualitative explanation of the effect.

## 4.3. Triaxial and *almost* prolate rotators

Typically, asteroids and comets have elongated shapes, and the above formulae derived for oblate bodies make a very crude approximation of the wobble of a realistic triaxial body. In the case of a triaxial rotator, with  $I_3 \geq I_2 \geq I_1$ , the solution to the Euler equations is

expressable in terms of elliptic functions. According to Jacobi (1882) and Legendre (1837), it will read, for  $\vec{J}^2 < 2 I_2 T_{kin}$ , as

$$\Omega_1 = \gamma \operatorname{dn}(\omega t, k^2) \quad , \quad \Omega_2 = \beta \operatorname{sn}(\omega t, k^2) \quad , \quad \Omega_3 = \alpha \operatorname{cn}(\omega t, k^2) \quad , \quad (4-29)$$

while for  $\vec{J}^2 > 2 I_2 T_{kin}$  it will be:

$$\Omega_1 = \gamma \operatorname{cn}(\omega t, k^2) \quad , \quad \Omega_2 = \beta \operatorname{sn}(\omega t, k^2) \quad , \quad \Omega_3 = \alpha \operatorname{dn}(\omega t, k^2) \quad . \quad (4-30)$$

Here the precession rate  $\omega$  and the parameters  $\alpha, \beta, \gamma$  and  $k$  are some algebraic functions of  $I_{1,2,3}, T_{kin}$  and  $\vec{J}^2$ . For example,  $k$  is expressed by

$$k = \sqrt{\frac{I_3 - I_2}{I_2 - I_1} \frac{\vec{J}^2 - 2I_1 T_{kin}}{2I_3 T_{kin} - \vec{J}^2}} \quad , \quad (4-31)$$

for (4-29), and by

$$k = \sqrt{\frac{I_2 - I_1}{I_3 - I_2} \frac{2I_3 T_{kin} - \vec{J}^2}{\vec{J}^2 - 2I_1 T_{kin}}} \quad , \quad (4-32)$$

for (4-30). In the limit of oblate symmetry (when  $I_2/I_1 \rightarrow 1$ ), solution (4-30) approaches (4-2), while the applicability region of (4-29) shrinks. Similarly, in the prolate-symmetry limit ( $(I_3 - I_2)/I_1 \rightarrow 0$ ) the applicability realm of (4-30) will become infinitesimally small. The easiest way of understanding this would be to consider, in the space  $\Omega_1, \Omega_2, \Omega_3$ , the angular-momentum ellipsoid  $\vec{J}^2 = I_1^2 \Omega_1^2 + I_2^2 \Omega_2^2 + I_3^2 \Omega_3^2$ . A trajectory described by the angular-velocity vector  $\vec{\Omega}$  in the space  $\Omega_1, \Omega_2, \Omega_3$  will be given by a line along which this ellipsoid intersects the kinetic-energy ellipsoid  $2 T_{kin} = I_1 \Omega_1^2 + I_2 \Omega_2^2 + I_3 \Omega_3^2$ , as on Fig.1. Through the relaxation process, the angular-momentum ellipsoid remains unchanged, while the kinetic-energy ellipsoid evolves as the energy dissipates. Thus, the fast process, nutation, will be illustrated by the (adiabatically) periodic motion of  $\vec{\Omega}$  along the line of ellipsoids' intersection; the slow process, relaxation, will be illustrated by the gradual shift of the moving vector  $\vec{\Omega}$  from one trajectory to another (Lamy & Burns 1972). On Fig.1, we present an angular-momentum ellipsoid for an almost prolate body whose angular momenta relate to one another as those of asteroid 433 Eros:  $1 \times 3 \times 3.05$  (Black et al. 1999). Suppose the initial energy was so high that  $\vec{\Omega}$  was moving along some trajectory close to the point A on Fig.1. This pole corresponds to rotation of the body about its minor-inertia axis. The trajectory described by  $\vec{\Omega}$  about A is almost circular and remains so until  $\vec{\Omega}$  approaches the separatrix<sup>18</sup>. This process will be described by solution (4-29). In the vicinity of separatrix, trajectories will become noticeably distorted. After the separatrix is crossed, librations will begin:  $\vec{\Omega}$  will be describing not an almost circular cone but an elliptic one. This process will be governed by solution (4-30). Eventually, in the closest vicinity of

---

<sup>18</sup>As we already mentioned above, this trajectory on Fig.1 being almost circular does not necessarily mean that the precession cone of the major-inertia axis about  $\vec{J}$  is circular or almost circular.

pole C, the precession will again become almost circular. (This point, though, will never be reached because the alignment of  $\vec{\Omega}$  along (or opposite to)  $\vec{\mathbf{J}}$  has a vanishing rate for small residual angles: at the end of the relaxation process the relaxation rate approaches zero, so that small-angle nutations can persist for long times.) Parameter  $k$  shows how far the tip of  $\vec{\Omega}$  is from the separatrix on Fig.1:  $k$  is zero in poles A and C, and is unity on the separatrix. It is defined by (4-31) when  $\vec{\Omega}$  is between point A and the separatrix, and by (4-32) when  $\vec{\Omega}$  is between the separatrix and point C. (For details see (Efroimsky 2000).)

Now suppose that the rotator is almost prolate, i.e., that point C is very closely embraced by the separatrices. If such a rotator gets even slightly disturbed, then, dependent upon the particular value of  $(I_3 - I_2)/I_3$  and upon the intensity of the occasional disturbance, the vector  $\vec{\Omega}$  will be either driven away from point C back to the separatrix, without crossing it, or will be forced to “jump” over it. Crossing of the separatrix may be accompanied by stochastic flipovers<sup>19</sup>. If we assume that  $(I_3 - I_2)/I_3$  is infinitesimally small, then the separatrix will approach point C infinitesimally close, and the faintest tidal interaction or collision will be able to push the vector  $\vec{\Omega}$  across the separatrix. In other words, an almost prolate body, during the most part of its history, will be precessing about its minimal-inertia axis.

If in the early stage of relaxation of an almost prolate ( $I_3 \approx I_2$ ) body the tip of vector  $\vec{\Omega}$  is near point A, then its slow departure away from A is governed by formula (9.22) in (Efroimsky 2000):

$$\begin{aligned} \frac{d \langle \sin^2 \theta \rangle}{dt} = & \\ & - \frac{4 \rho^2 \vec{\mathbf{J}}^2}{\mu Q(\omega)} (I_3 - I_1) (1 - \langle \sin^2 \theta \rangle) \left\{ \omega S_1 [2 \langle \sin^2 \theta \rangle - 1 - \right. \\ & \left. - \frac{1}{2} \frac{I_3 - I_2}{I_2 - I_1} \frac{I_1}{I_3} (1 - \langle \sin^2 \theta \rangle)] - \right. \\ & \left. - \omega S_0 \frac{2 I_1}{I_3} (1 - \langle \sin^2 \theta \rangle) + 2 \omega S_2 \frac{Q(2\omega)}{Q(\omega)} \frac{2 I_1}{I_3} (1 - \langle \sin^2 \theta \rangle) \right\}. \end{aligned} \quad (4-33)$$

where

$$\omega = \sqrt{\frac{(2 I_3 T_{kin} - \vec{\mathbf{J}}^2) (I_2 - I_1)}{I_1 I_2 I_3}} \approx \frac{|\vec{\mathbf{J}}|}{I_1} \sqrt{\frac{(I_3 - I_1) (I_2 - I_1)}{I_2 I_3}} \sqrt{2 \langle \sin^2 \theta \rangle - 1}, \quad (4-34)$$

$\theta$  is the angle between the angular-momentum vector  $\vec{\mathbf{J}}$  and the major-inertia axis  $\mathbf{3}$ ;  $S_{0,1,2}$  are some geometrical factors ( $S_0 = 0$  in the case of  $I_2 = I_3$ ), and  $\langle \dots \rangle$  symbolises an

---

<sup>19</sup>The flipovers are unavoidable if dissipation of the kinetic energy through one precession cycle is less than a typical energy of an occasional interaction (a tidal-force-caused perturbation, for example).

average over the precession cycle. For  $\langle \cos^2\theta \rangle$  not exceeding  $\approx 1/7$ , this equation has an exponentially decaying solution. For  $c/a = 0.6$  that solution will read:

$$\Delta t \approx (-\Delta\langle\theta\rangle) \times 0.08 \frac{\mu Q}{a^2 \Omega_0^3 \rho} . \quad (4-35)$$

Comparing this with (4-22), we see that at this stage the relaxation is about 15 times faster than in the case of an oblate body.

During the later stage, when  $\vec{\Omega}$  gets close to the separatrix, all the higher harmonics will come into play, and our estimate will become invalid. How do the higher harmonics emerge? Plugging of (4-29) or (4-30) into (4-12) will give an expression for the acceleration of an arbitrary point inside the body. Due to (1-20), that expression will yield formulae for the stresses. These formulae will be similar to (4-13 - 4-16), but will contain elliptic functions instead of the trigonometric functions. In order to plug these formulae for  $\sigma_{ij}$  into (1-22), they must first be squared and averaged over the precession cycle. For a rectangular prizm  $2a \times 2b \times 2c$ , a direct calculation carried out in (Efroimsky 2000) gives:

$$\langle \sigma_{xx}^2 \rangle = \frac{\rho^2}{4} (1 - Q)^2 \beta^4 (x^2 - a^2)^2 \Xi_1 , \quad (4-36)$$

$$\langle \sigma_{yy}^2 \rangle = \frac{\rho^2}{4} (S + Q)^2 \beta^4 (y^2 - b^2)^2 \Xi_1 , \quad (4-37)$$

$$\langle \sigma_{zz}^2 \rangle = \frac{\rho^2}{4} (1 - S)^2 \beta^4 (z^2 - c^2)^2 \Xi_1 , \quad (4-38)$$

$$\langle (Tr \sigma)^2 \rangle = \frac{\rho^2}{4} \beta^4 \{ (1 - Q)(x^2 - a^2)^2 + (S + Q)(y^2 - b^2) + (1 - S)(z^2 - c^2) \}^2 \Xi_1 , \quad (4-39)$$

$$\langle \sigma_{xy}^2 \rangle = \frac{\rho^2}{4} \{ (\beta\gamma + \alpha\omega k^2)(y^2 - b^2) + (\beta\gamma - \alpha\omega k^2)(x^2 - a^2) \}^2 \Xi_2 , \quad (4-40)$$

$$\langle \sigma_{xz}^2 \rangle = \frac{\rho^2}{4} \{ (\beta\omega + \alpha\gamma)(z^2 - c^2) + (\beta\omega - \alpha\gamma)(x^2 - a^2) \}^2 \Xi_3 , \quad (4-41)$$

$$\langle \sigma_{yz}^2 \rangle = \frac{\rho^2}{4} \{ (\alpha\beta + \omega\gamma)(z^2 - c^2) + (\alpha\beta - \omega\gamma)(y^2 - b^2) \}^2 \Xi_4 , \quad (4-42)$$

where  $Q$  and  $S$  are some combinations of  $I_1, I_2, I_3$ , defined by formula (2.8) in (Efroimsky 2000). Factors  $\Xi_{1,2,3,4}$  stand for averaged powers of the elliptic functions:

$$\begin{aligned} \Xi_1 &\equiv \langle (sn^2(u, k^2) - \langle sn^2(u, k^2) \rangle)^2 \rangle = \\ &= \langle sn^4(u, k^2) \rangle - \langle sn^2(u, k^2) \rangle^2 , \end{aligned} \quad (4-43)$$

$$\begin{aligned} \Xi_2 &\equiv \langle (sn(u, k^2) cn(u, k^2) - \langle sn(u, k^2) cn(u, k^2) \rangle)^2 \rangle = \\ &= \langle sn^2(u, k^2) cn^2(u, k^2) \rangle - \langle sn(u, k^2) cn(u, k^2) \rangle^2 , \end{aligned} \quad (4-44)$$

$$\begin{aligned}\Xi_3 &\equiv \langle (cn(u, k^2) dn(u, k^2) - \langle cn(u, k^2) dn(u, k^2) \rangle)^2 \rangle = \\ &= \langle cn^2(u, k^2) dn^2(u, k^2) \rangle - \langle cn(u, k^2) dn(u, k^2) \rangle^2 ,\end{aligned}\quad (4-45)$$

$$\begin{aligned}\Xi_4 &\equiv \langle (sn(u, k^2) dn(u, k^2) - \langle sn(u, k^2) dn(u, k^2) \rangle)^2 \rangle = \\ &= \langle sn^2(u, k^2) dn^2(u, k^2) \rangle - \langle sn(u, k^2) dn(u, k^2) \rangle^2 ,\end{aligned}\quad (4-46)$$

where averaging implies:

$$\langle \dots \rangle \equiv \frac{1}{\tau} \int_0^\tau \dots du , \quad (4-47)$$

$\tau$  being the mutual period of  $sn$  and  $cn$  and twice the period of  $dn$  :

$$\tau = 4 K(k^2) \equiv 4 \int_0^{\pi/2} (1 - k^2 \sin^2 \psi)^{-1/2} d\psi . \quad (4-48)$$

The origin of expressions (4-43 - 4-46) can be traced from formulae (8.4, 8.6 - 8.13) in (Efroimsky 2000). For example, expression (4-11), that gives acceleration of an arbitrary point inside the body, contains term  $sn^2(\omega t, k^2)$  . (Indeed, one of the components of the angular velocity is proportional to  $sn(\dots)$ , while the centripetal part of the acceleration is a quadratic form of the angular-velocity components.) The term  $sn^2(\omega t, k^2)$  in the formula for acceleration yields a similar term in the expression for  $\sigma_{xx}$  . For this reason expression (8.6) in (Efroimsky 2000), that gives the **time-dependent part** of  $\sigma_{xx}$  , contains  $sn^2(\dots) - \langle sn^2(\dots) \rangle$  , wherefrom (4-43) ensues.

Now imagine that in the formulae (4-36 - 4-42) the elliptic functions are presented by their series expansions over sines and cosines (Abramovitz & Stegun 1965):

$$sn(\omega t, k^2) = \frac{2\pi}{k K} \sum_{n=1}^{\infty} \frac{q^{n/2}}{1 - q^n} \sin(\omega_n t) , \quad (4-49)$$

$$cn(\omega t, k^2) = \frac{2\pi}{k K} \sum_{n=1}^{\infty} \frac{q^{n/2}}{1 + q^n} \cos(\omega_n t) , \quad (4-50)$$

$$dn(\omega t, k^2) = \frac{\pi}{2 K} + \frac{2\pi}{K} \sum_{n=0}^{\infty} \frac{q^{n/2}}{1 + q^n} \cos(\omega_n t) , \quad (4-51)$$

where

$$\omega_n = n \omega \pi / (2K(k^2)) , \quad q = \exp(-\pi K(k'^2)/K(k^2)) , \quad k'^2 \equiv 1 - k^2 \quad (4-52)$$

and the function  $K(k^2)$  is the complete elliptic integral of the first kind (see (4-48) or (4-57)). A star in the superscript denotes a sum over odd  $n$ 's only; a double star stands for a sum over even  $n$ 's. Insertion of (4-49-4-51) into (4-36-4-42) will produce, after squaring of  $sn$ ,  $cn$ ,  $dn$ , an infinite amount of terms like  $\sin^2(\omega_n t)$  and  $\cos^2(\omega_n t)$ , along with an infinite amount of cross terms. The latter will be removed after averaging over the precession period, while the former will survive for all  $n$ 's and will average to 1/2. Integration over the volume will then lead to an expression like (1-16), with an infinite amount of contributions  $\langle W_n \rangle$  originating from all  $\omega_n$ 's,  $n = 1, \dots, \infty$ . This is how an infinite amount of overtones comes into play. These overtones are multiples not of precession rate  $\omega$  but of the "base frequency"  $\omega_1 \equiv \omega\pi/(2K(k^2))$  which is lower than  $\omega$ . Hence the stresses and strains contain not only Fourier components oscillating at frequencies higher than the precession rate, but also components oscillating at frequencies lower than  $\omega$ . This is a very unusual and counterintuitive phenomenon.

The above series (called "nome expansions") typically converge very quickly, for  $q \ll 1$ . Note, however, that  $q \rightarrow 1$  at the separatrix. Indeed, on approach to the separatrix we have:  $k \rightarrow 1$ , wherefrom  $K(k^2) \rightarrow \infty$ ; therefore  $q \rightarrow 1$  and  $\omega_n \rightarrow 0$  (see eqn. (4-52)). The period of rotation (see (4-48)) becomes infinite. (This is the reason why near-separatrix states can mimic the principal one.)

Paper (Efroimsky 2000), addressed relaxation in the vicinity of poles. This case corresponds to  $k \ll 1$ . For this reason we used, instead of (4-49 - 4-51), trivial approximations  $\omega_1 \approx \omega$ ,  $sn(\omega t, k^2) \approx \sin(\omega t)$ ,  $cn(\omega t, k^2) \approx \cos(\omega t)$ ,  $dn(\omega t, k^2) \approx 1$ . These approximations, along with (4-36 - 4-46) enabled us to assume that the terms  $\sigma_{xz}^2$  and  $\sigma_{yz}^2$  in (4-6) are associated with the principal frequency  $\omega$ , while  $\langle \sigma_{xx}^2 \rangle$ ,  $\langle \sigma_{yy}^2 \rangle$ ,  $\langle \sigma_{zz}^2 \rangle$ ,  $\langle (Tr \sigma)^2 \rangle$  and  $\sigma_{xy}^2$  are associated with the second harmonic  $2\omega$ . No harmonics higher than second appeared in that case. However, if we move away from the poles, parameter  $k$  will no longer be small (and will be approaching unity as we approach the separatrix). Hence we shall have to take into account all terms in (4-49 - 4-51) and, as a result, shall get an infinite amount of contributions from all  $\omega_n$ 's in (1-22 - 1-16). Thus we see that the problem is very highly nonlinear. It is nonlinear even though the properties of the material are assumed linear (strains  $\epsilon$  are linear functions of stresses  $\sigma$ ). Retrospectively, the nonlinearity originates because the dissipation rate (and, therefore, the relaxation rate) is proportional to the averaged (over the cycle) elastic energy stored in the body experiencing precession-caused alternating deformations. The average elastic energy is proportional to  $\langle \sigma \epsilon \rangle$ , i.e., to  $\langle \sigma^2 \rangle$ . The stresses are proportional to the components of the acceleration, that are quadratic in the components of the angular velocity (4-29 - 4-30). All in all, the relaxation rate is a quartic form of the angular-velocity components that are expressed by the elliptic functions (4-49 - 4-51).

A remarkable fact about this nonlinearity is that it produces oscillations of stresses and strains not only at frequencies higher than the precession frequency  $\omega$  but also at frequencies lower than  $\omega$ . This is evident from formula (4-52): the closer we get to the separatrix (i.e.,

the closer  $k^2$  gets to unity), the smaller the factor  $\pi/(2K)$ , and the more lower-than- $\omega$  frequencies emerge.

A quantitative study of near-separatrix wobble will imply attributing extra factors of  $\omega_n/Q(\omega_n)$  to each term of the series (1-16) and investigating the behaviour of the resulting series (1-17). This study will become the topic of our next paper. Nevertheless, some qualitative judgement about the near-separatrix behaviour can be made even at this point.

For the calculation of the dissipation rate (1-17), the value of the average elastic energy  $\langle W \rangle$  given by the sum (1-16) is of no use (unless each of its terms is multiplied by  $\omega_n/Q(\omega_n)$  and plugged into (1-17)). For this reason, the values of the terms  $\langle \sigma_{ij}^2 \rangle$  entering (1-22) are of no practical value either; only their expansions obtained by plugging (4-49 - 4-51) into (4-36 - 4-46) do matter. Nonetheless, let us evaluate  $\langle W \rangle$  near the separatrix. To that end, one has to calculate all  $\langle \sigma_{ij}^2 \rangle$ 's by evaluating (4-43 - 4-46). Direct integration in (4-43 - 4-47) leads to:

$$\Xi_1 = \frac{1}{3k^4} \left\{ k^2 - 1 + \frac{2E}{K} (2 - k^2) - 3 \left( \frac{E}{K} \right)^2 \right\} , \quad (4-53)$$

$$\Xi_2 = \frac{1}{3k^4} \left\{ 2 (k^2 - 1) + \frac{E}{K} (-2 - 5k^2) \right\} , \quad (4-54)$$

$$\Xi_3 = \frac{1}{3k^2} \left\{ \frac{E}{K} (1 + k^2) + (k^2 - 1) \right\} , \quad (4-55)$$

$$\Xi_4 = \frac{1}{3k^2} \left\{ \frac{E}{K} (2k^2 - 1) + (1 - k^2) \right\} , \quad (4-56)$$

$K$  and  $E$  being abbreviations for the complete elliptic integrals of the 1st and 2nd kind:

$$K \equiv K(k^2) \equiv \int_0^{\pi/2} (1 - k^2 \sin^2 \psi)^{-1/2} d\psi , \quad (4-57)$$

$$E \equiv E(k^2) \equiv \int_0^{\pi/2} (1 - k^2 \sin^2 \psi)^{1/2} d\psi .$$

In the limit of  $k \rightarrow 1$ , the expression for  $K$  will diverge and all  $\Xi_i$  will vanish. Then all  $\langle \sigma_{ij}^2 \rangle$  will also become nil, and so will  $\langle W \rangle$ . As all the inputs  $\langle W(\omega_n) \rangle$  in (1-17) are nonnegative, each of them will vanish too. Hence the relaxation slows down near the separatrix. Moreover, it appears to completely halt on it. How trustworthy is this conclusion? On the one hand, it might have been guessed simply from looking at (4-48): since for  $k \rightarrow 1$  the period  $4K(k^2)$  diverges (or, stated differently, since the frequencies  $\omega_n$  in (4-52) approach zero for each fixed  $n$ , then all the averages may vanish). On the other

hand, though, the divergence of the period undermines the entire averaging procedure: for  $\tau \rightarrow \infty$ , expression (1-13) becomes pointless. Let us have a look at the expressions for the angular-velocity components near the separatrix. According to (Abramovits & Stegun 1965), these expressions may be expanded into series over small parameter  $(1 - k^2)$ :

$$\begin{aligned} \Omega_1 &= \gamma \operatorname{dn}(\omega t, k^2) = \gamma \left\{ \operatorname{sech}(\omega t) + \right. \\ &+ \left. \frac{1}{4} (1 - k^2) [\sinh(\omega t) \cosh(\omega t) + \omega t] \operatorname{sech}(\omega t) \tanh(\omega t) \right\} + O((1 - k^2)^2) \quad , \quad (4-58) \end{aligned}$$

$$\begin{aligned} \Omega_2 &= \beta \operatorname{sn}(\omega t, k^2) = \beta \left\{ \tanh(\omega t) + \right. \\ &+ \left. \frac{1}{4} (1 - k^2) [\sinh(\omega t) \cosh(\omega t) - \omega t] \operatorname{sech}^2(\omega t) \right\} + O((1 - k^2)^2) \quad , \quad (4-59) \end{aligned}$$

$$\Omega_3 = \alpha \operatorname{cn}(\omega t, k^2) = \alpha \left\{ \operatorname{sech}(\omega t) - \right. \quad (4-60)$$

$$\left. - \frac{1}{4} (1 - k^2) [\sinh(\omega t) \cosh(\omega t) - \omega t] \operatorname{sech}(\omega t) \tanh(\omega t) \right\} + O((1 - k^2)^2) \quad . \quad (4-61)$$

These expansions will remain valid for small  $k^2$  up to the point  $k^2 = 1$ , inclusively. It doesn't mean, however, that in these expansions we may take the limit of  $t \rightarrow \infty$ . (This difficulty arises because this limit is not necessarily interchangeable with the infinite sum of terms in the above expansions.) Fortunately, though, for  $k^2 = 1$ , the limit expressions

$$\Omega_1 = \gamma \operatorname{dn}(\omega t, 1) = \gamma \operatorname{sech}(\omega t) \quad , \quad (4-62)$$

$$\Omega_2 = \beta \operatorname{sn}(\omega t, 1) = \beta \tanh(\omega t) \quad , \quad (4-63)$$

$$\Omega_3 = \alpha \operatorname{cn}(\omega t, 1) = \alpha \operatorname{sech}(\omega t) \quad (4-64)$$

make an exact solution to (1-4). Thence we can see what happens to vector  $\vec{\Omega}$  when its tip is right on the separatrix. If there were no inelastic dissipation, the tip of vector  $\vec{\Omega}$  would be slowing down while moving along the separatrix, and will come to halt at one of the middle-inertia homoclinic unstable poles (though it would formally take  $\vec{\Omega}$  an infinite time to get there, because  $\Omega_1$  and  $\Omega_3$  will be approaching zero as  $\sim \exp(-\omega t)$ ). When  $\vec{\Omega}$  gets sufficiently close to the homoclinic point, the precession will slow down so that an observer would get an impression that the body is in a simple-rotation state. In reality, some tiny dissipation will still be present even for very slowly evolving  $\vec{\Omega}$ . It will be present because this slow evolution will cause slow changes in the stresses and strains. The dissipation will result in a further decrease of the kinetic energy, that will lead to a change in the value of  $k^2$  (which is a function of energy; see (4-31) and (4-32)). A deviation of  $k^2$  away from



unity will imply a shift of  $\vec{\Omega}$  away from the separatrix towards pole C. So, the separatrix eventually will be crossed, and the near-separatrix slowing-down does NOT mean a complete halt.

This phenomenon of near-separatrix slowing-down (that we shall call **lingering effect**) is not new. In a slightly different context, it was mentioned by Chernous'ko (1968) who investigated free precession of a tank filled with viscous liquid and proved that, despite the apparent trap, the separatrix is crossed within a finite time. Recently, the capability of near-intermediate-axis rotational states to mimic simple rotation was pointed out by Samarasinha, Mueller & Belton (1999) with regard to comet Hale-Bopp.

We, thus, see that the near-separatrix dissipational dynamics is very subtle, from the mathematical viewpoint. On the one hand, more of the higher overtones of the base frequency will become relevant (though the base frequency itself will become lower, approaching zero as the angular-velocity vector approaches the separatrix). On the other hand, the separatrix will act as a (temporary) trap, and the duration of this lingering is yet to be estimated.

One should, though, always keep in mind that a relatively weak push can help the spinning body to cross the separatrix trap. So, for many rotators (at least, for the smallest ones, like cosmic-dust grains) the observational reality near separatrix will be defined not so much by the mathematical sophistries but rather by high-order physical effects: the solar wind, magnetic field effects, etc... In the case of a macroscopic rotator, a faint tidal interaction or a collision with a smaller body may help to cross the separatrix.

## 5. APPLICATION TO WOBBLING ASTEROIDS

### 5.1. Relaxation Rates of Comets and Asteroids

Knowledge of the alignment rate  $\dot{\theta}$  as a function of the precession-cone half-angle  $\theta$  enables one not only to write down a typical relaxation time but to calculate the entire dynamics of the process. In particular, suppose the observer is capable of measuring the precession-cone half-angle  $\theta$  with an error  $\delta$ . This observer will then compute, by means of (4-22), the time needed for the body to change its residual half-angle from  $\theta$  to  $\theta - \Delta\theta$ , for  $\Delta\theta > \delta$ . This time will then be compared with the results of his further measurements. Below we shall show that such measurements will soon become possible for spacecraft-based observation means.

First, let us find a typical relaxation time, i.e., a time span necessary for the major-inertia axis to shift considerably toward alignment with  $\mathbf{J}$ . This time may be defined as:

$$t_r \equiv \int_{\theta_0}^{\delta} \frac{d\theta}{d\theta/dt} \quad , \quad (5-1)$$

$\theta_0$  being the initial half-angle of the precession cone ( $\theta_0 < \pi/2$ ), and  $\delta$  being the minimal experimentally-recognisable value of  $\theta$ . A finite  $\delta$  will prevent the “slow-finish” divergency.

A particular choice of  $\theta_0$  and  $\delta$  will lead to an appropriate numerical factor in the final expression for  $t_r$ . As explained in (Efroimsky 2001),  $t_r$  is not very sensitive to the choice of angle  $\theta_0$ , as long as this angle is not too small. This weak dependence upon the initial angle is natural since our approach accounts for the divergence at small angles (“exponentially slow finish”) and ignores the “slow start”. Therefore one can take, for a crude estimate,

$$\theta_0 = \pi/2 \quad . \quad (5-2)$$

For  $t_r$  it would give almost the same result as, say,  $\pi/3$  or  $\pi/4$ . A choice of  $\delta$  must be determined exclusively by the accuracy of the observation technique:  $\delta$  is such a minimally recognizable angle that precession within a cone of half-angle  $\delta$  or less cannot be detected. Ground-based photometers measure the lightcurve-variation amplitude that is approximately proportional to the variation in the cross-sectional area of the wobbling body. In such sort of experiments the relative error is around  $0.01$ . In other words, only deviations from one revolution to the next exceeding  $0.01 \text{ mag}$  may be considered real. This corresponds to precession-cone half-angles  $\delta \approx 10^\circ$  or larger (Steven Ostro, private communication). Ground-based radars have a much sharper resolution and can grasp asteroid-shape details as fine as  $10 \text{ m}$ . This technique may reveal precession at half-angles of about 5 degrees. NEAR-type missions potentially may provide an accuracy of  $0.01^\circ$  (Miller et al. 1999). For a time being, we would lean to a conservative estimate

$$\delta = 6^\circ \quad , \quad (5-3)$$

though we hope that within the coming years this limit may be reduced by three orders due to advances in the spacecraft-borne instruments.

Remarkably,  $t_r$  is not particularly sensitive to the half-sizes’ ratio  $c/a$  either, when this ratio is between 0.5 - 0.9 (which is the case for realistic asteroids, comets and many spacecraft). Our formulae give:

$$t_{(our \ result)} \approx (1 - 2) \frac{\mu Q}{\rho a^2 \Omega_0^3} \quad for \quad \theta_0 \approx (2 - 3) \delta = 12 - 18^\circ \quad ;$$

$$t_{(our \ result)} \approx (3 - 4) \frac{\mu Q}{\rho a^2 \Omega_0^3} \quad for \quad \theta_0 \approx \pi/4 \quad ; \quad (5-4)$$

$$t_{(our \ result)} \approx (4 - 5) \frac{\mu Q}{\rho a^2 \Omega_0^3} \quad for \quad \theta_0 \lesssim \pi/2 \quad .$$

(Mind though that, according to (4-25),  $\theta$  should not approach  $\pi/2$  too close.) To compare our results with a preceding study, recall that according to Burns & Safronov (1973)

$$t_{(B \ \& \ S)} \approx 100 \frac{\mu Q}{\rho a^2 \Omega_0^3} \quad . \quad (5-5)$$

The numerical factor in Burns & Safronov’s formula is about 100 for objects of small oblateness, i.e., for comets and for many asteroids. (For objects of irregular shapes Burns and Safronov suggested a factor of about 20 in place of 100.)

This numerical factor is the only difference between our formula and that of Burns & Safronov. This difference, however, is quite considerable: for small residual half-angles  $\theta$ , our value of the relaxation time is two orders smaller than that predicted by Burns & Safronov. For larger residual half-angles, the times differ by a factor of several dozens. We see that the effectiveness of the inelastic relaxation was much underestimated by our predecessors. There are three reasons for this underestimation. The first reason is that our calculation was based on an improved solution to the boundary-value problem for stresses. Expressions (4-13) - (4-16) show that an overwhelming share of the deformation (and, therefore, of the inelastic dissipation) is taking place in the depth of the body. This is very counterintuitive, because on a heuristic level the picture of precession would look like this: a centrifugal bulge, with its associated strains, wobbles back and forth relative to the body as  $\Omega$  moves through the body during the precession period. This naive illustration would make one think that most of the dissipation is taking place in the shallow regions under and around the bulge. It turns out that in reality most part of the deformation and dissipation takes place deep beneath the bulge (much like in the simple example with the liquid planet, that we provided in subsection 1.5. The second, most important, reason for our formulae giving smaller values for the relaxation time is that we have taken into account the second harmonic. In many rotational states this harmonic turns to be a provider of the main share of the entire effect. In the expression  $(63(c/a)^4 \cot^2 \theta + 20)$  that is a part of formula (4-22), the term  $63(c/a)^4 \cot^2 \theta$  is due to the principal frequency, while the term 20 is due to the second harmonic<sup>20</sup>. For  $c/a$  belonging to the realistic interval  $0.5 - 0.9$ , the second harmonic contributes (after integration from  $\theta_0$  through  $\delta$ ) a considerable input in the entire effect. This input will be of the leading order, provided the initial half-angle  $\theta_0$  is not too small (not smaller than about  $30^\circ$ ). In the case of a small initial half-angle, the contribution of the second mode is irrelevant. Nevertheless it is the small-angle case where the discrepancy between our formula and (5-5) becomes maximal. The estimate (5-5) for the characteristic time of relaxation was obtained in Burns & Safronov (1973) simply as a reciprocal to their estimate for  $\dot{\theta}$ ; it ignores any dependence upon the initial angle, and thus gives too long times for small angles. The dependence of the dissipation rate of the values of  $\theta$  is the third of the reasons for our results being so different from the early estimate (5-5).

Exploration of this, third, reason may give us an important handle on observation of asteroid relaxation. It follows from (4-22) that a small decrease in the precession-cone half-angle,  $-\Delta\theta$ , will be performed during the following period of time:

$$\Delta t = (-\Delta\theta) \frac{2^4}{3} \frac{[1 + (c/a)^2]^4}{63 (c/a)^4 \cot^2 \theta + 20} \frac{1}{\sin^3 \theta} \frac{\mu Q}{a^2 \Omega_0^3 \rho} . \quad (5-6)$$

---

<sup>20</sup>For calculational details, see Lazarian & Efroimsky (1999).

For asteroids composed of solid silicate rock, the density may be assumed  $\rho \approx 2.5 \times 10^3 \text{ kg/m}^3$ , while the product in the numerator should be  $\mu Q \approx 1.5 \times 10^{13} \text{ dyne/cm}^2 = 1.5 \times 10^{12} \text{ Pa}$  as explained in Efroimsky & Lazarian (2000). Burns & Safronov suggested a much higher value of  $3 \times 10^{14} \text{ dyne/cm}^2 = 3 \times 10^{13} \text{ Pa}$ , value acceptable within the terrestrial seismology but, probably, inapplicable to asteroids.

For asteroids composed of friable materials, Harris (1994) suggests the following values:  $\rho \approx 2 \times 10^3 \text{ kg/m}^3$  and  $\mu Q \approx 5 \times 10^{12} \text{ dyne/cm}^2 = 5 \times 10^{11} \text{ Pa}$ . Naturally, this value is lower than those appropriate for solid rock (Efroimsky & Lazarian 2000), but in our opinion it is still too high for a friable medium. Harris borrowed the aforementioned value from preceding studies of Phobos (Yoder 1982). Mind, though, that Phobos may consist not only of rubble: it may have a solid component in the centre. In this case, a purely rubble-pile asteroid may have a lower  $\mu Q$  than suggested by Harris. Anyway, as a very conservative estimate for a rubble-pile asteroid, we shall take the value suggested by Harris.

As for the geometry, let, for example,  $\theta = \pi/3$  and  $c/a = 0.6$ . Then

$$\Delta t = (-\Delta\theta) 1.2 \frac{\mu Q}{a^2 \Omega_0^3 \rho} . \quad (5-7)$$

If we measure time  $\Delta t$  in years, the revolution period  $T = 2\pi/\Omega_0$  in hours, the maximal half-size  $a$  in kilometers, and  $\theta$  in angular degrees ( $\Delta\theta = \Delta\theta^\circ \times 1.75 \times 10^{-2}$ ), our formula (5-6) will yield:

$$\Delta t_{(years)} = (-\Delta\theta^\circ) \times 1.31 \times 10^{-7} \frac{\mu Q}{\rho} \frac{T_{(hours)}^3}{a_{(km)}^2} = 0.33 \frac{T_{(hours)}^3}{a_{(km)}^2} , \quad (5-8)$$

where we accepted Harris' values of  $\mu Q = 5 \times 10^{11} \text{ Pa}$  and  $\rho = 2 \times 10^3 \text{ kg/m}^3$ , and the angular resolution of spacecraft-based devices was assumed to be as sharp as  $|\Delta\theta| = 0.01^\circ$ , according to Miller et al. (1999).

## 5.2. Parameters of Well-Consolidated Asteroids

Values of the parameters that appear in the above formulae depend both upon the body temperature and upon the wobble frequency. The temperature-, pressure- and frequency-caused variations of the density  $\rho$  are tiny and may be neglected. This way, we can use the (static) densities appropriate to the room temperature and pressure:  $\rho^{(silicate)} \approx 2500 \text{ kg m}^{-3}$  and  $\rho^{(carbon)} \approx 2000 \text{ kg m}^{-3}$ .

As for the adiabatic shear modulus  $\mu$ , tables of physical quantities would provide its values at room temperature and atmospheric pressure, and for quasistatic regimes solely. As for the possible frequency-related effects in materials (the so-called ultrasonic attenuation), these become noticeable only at frequencies higher than  $10^8 \text{ Hz}$  (see section 17.7 in Nowick and Berry 1972). Another fortunate circumstance is that the pressure-dependence of the

elastic moduli is known to be weak (Ahrens 1995). Besides, the elastic moduli of solids are known to be insensitive to temperature variations, as long as these variations are far enough from the melting point. The value of  $\mu$  may increase by several percent when the temperature drops from room temperature to  $10\text{ K}$ . Dislocations don't affect the elastic moduli either. Solute elements have very little effect on moduli in quantities up to a few percent. Besides, the moduli vary linearly with substitutional impurities (in which the atoms of the impurity replace those of the hosts). However hydrogen is not like that: it enters the interstices between the atoms of the host, and has marginal effect on the modulus. As for the role of the possible porosity, the elastic moduli scale as the square of the relative density. For porosities up to about 20 % , this is not of much relevance for our estimates.

According to Ryan and Blevins (1987), for both carbonaceous and silicate rocks one may take the shear-modulus value  $\mu \approx 10^{10}\text{ Pa}$  .

Theoretical estimation of the  $Q$ -factor for asteroids is difficult. As well known from seismology, the  $Q$ -factor bears a pronounced dependence upon: the chemical composition, graining, frequency, temperature, and confining pressure. It is, above all, a steep function of the humidity which presumably affects the interaction between grains. The  $Q$ -factor is less sensitive to the porosity (unless the latter is very high); but it greatly depends upon the amount and structure of cracks, and generally upon the mechanical nature of the aggregate. Whether comets and asteroids are loose aggregates or solid chunks remains unknown. We shall address this question in the next subsection. For now, we shall assume that the body is not a loosely connected aggregate but a solid rock (possibly porous but nevertheless well-consolidated), and shall try to employ some knowledge available on attenuation in the terrestrial and lunar crust.

We are in need of the values of the quality factors for silicate and carbonateous rocks. We need these at the temperatures about 150 K, , zero confining pressure, frequencies appropriate to asteroid precession ( $10^{-6} - 10^{-4}\text{ Hz}$ ), and (presumably!) complete lack of moisture.

Much data on the behaviour of  $Q$ -factors is presented in the seismological literature. Almost all of these measurements have been made under high temperatures (from several hundred up to 1500 Celsius), high confining pressures (up to dozens of MPa), and unavoidably in the presence of humidity. Moreover, the frequencies were typically within the range from dozens of  $k\text{Hz}$  up to several  $M\text{Hz}$ . Only a very limited number of measurements have been performed at room pressure and temperature, while no experiments at all have been made thus far with rocks at low temperatures (dozens of  $K$  ). The information about the role of humidity is extremely limited. Worst of all, only a few experiments were made with rocks at the lowest seismological frequencies ( $10^{-3} - 10^{-1}\text{ Hz}$ ), and none at frequencies between  $10^{-6}$  and  $10^{-2}\text{ Hz}$ , though some indirectly achieved data are available (see Burns 1977, Burns 1986, Lambeck 1980, and references therein).

It was shown by Tittman et al. (1976) that the  $Q$ -factor of about 60 measured under ambient conditions on an as-received lunar basalt was progressively increased ultimately to

about 3300 as a result of outgassing under hard vacuum. The latter number will be our starting point. The measurements were performed by Tittman et al. at 20  $kHz$  frequency, room temperature and no confining pressure. How might we estimate the values of  $Q$  for the lunar basalt, appropriate to the lowest frequencies and temperatures?

As for the frequency-dependence, it is a long-established fact (e.g., Jackson 1986, Karato 1998) that  $Q \sim \omega^\alpha$  with  $\alpha$  around 0.25. This dependence reliably holds for all rocks within a remarkably broad band of frequencies: from hundreds of  $kHz$  down to  $10^{-1}Hz$ . Very limited experimental data are available for frequencies down to  $10^{-3}Hz$ , and none below this threshold. Keep in mind that  $\alpha$  being close to 0.25 holds well only at temperatures of several hundred Celsius and higher, while at lower temperatures  $\alpha$  typically decreases to 0.1 and less.

As regards the temperature-dependence, there is no consensus on this point in the geological literature. Some authors (Jackson 1986) use a simple rule:

$$Q \sim \omega^\alpha \exp(A^*/RT) \quad , \quad (5-9)$$

$A^*$  being the apparent activation energy. A more refined treatment takes into account the interconnection between the frequency- and temperature-dependences. Briefly speaking, since the quality factor is dimensionless, it must retain this property despite the exponential frequency-dependence. This may be achieved only in the case that  $Q$  is a function not of the frequency *per se* but of a dimensionless product of the frequency by the typical time of defect displacement. The latter exponentially depends upon the activation energy, so that the resulting dependence will read (Karato 1998):

$$Q \sim [\omega \exp(A^*/RT)]^\alpha \quad , \quad (5-10)$$

where  $A^*$  may vary from 150 - 200  $kJ/mol$  (for dunite and polycrystalline forsterite) up to 450  $kJ/mol$  (for olivine). This interconnection between the frequency- and temperature-dependences tells us that whenever we lack a pronounced frequency-dependence, the temperature-dependence is absent too. It is known, for example (Brennan 1981) that at room temperature and pressure, at low frequencies ( $10^{-3} - 1 Hz$ ) the shear  $Q$ -factor is almost frequency-independent for granites and (except some specific peak of attenuation, that makes  $Q$  increase twice) for basalts. It means that within this range of frequencies  $\alpha$  is small (like 0.1, or so), and  $Q$  may be assumed almost temperature-independent too.

Presumably, the shear  $Q$ -factor, reaching several thousand at 20  $kHz$ , descends, in accordance with (5-10), to several hundred when the frequency decreases to several  $Hz$ . Within this band of frequencies, we should use the power  $\alpha \approx 0.25$ , as well known from seismology. When we go to lower frequencies (from several  $Hz$  to the desirable  $10^{-6} - 10^{-4} Hz$ ), the  $Q$ -factor will descend at a slower pace: it will obey (5-10) with  $\alpha < 0.1$ . Low values of  $\alpha$  at low frequencies are mentioned in Lambeck (1980) and in Lambeck (1988)<sup>21</sup>.

---

<sup>21</sup>See also Knopoff (1963) where a very slow and smooth frequency-dependence of  $Q$  at low frequencies is pointed out.

The book by Lambeck contains much material on the  $Q$ -factor of the Earth. Unfortunately, we cannot employ the numbers that he suggests, because in his book the quality factor is defined for the Earth as a whole. Physically, there is a considerable difference between the  $Q$ -factors emerging in different circumstances, like for example, between the effective tidal  $Q$ -factor<sup>22</sup> and the  $Q$ -factor of the Chandler wobble). In regard to the latter, Lambeck (1988) refers, on page 552, to Okubo (1982) who suggested that for the Chandler wobble  $50 < Q < 100$ . Once again, this is a value for the Earth as a whole, with its viscous layers, etc. We cannot afford using these numbers for a fully solid asteroid.

Brennan (1981) suggests for the shear  $Q$ -factor the following values<sup>23</sup>:  $Q_{(shear)}^{(granite)} \approx 250$ ,  $Q_{(shear)}^{(basalt)} \approx 500$ . It would be tempting to borrow these values<sup>24</sup>, if not for one circumstance: as is well known, absorption of only several monolayers of a saturant may dramatically decrease the quality factor. We have already mentioned this in respect to moisture, but the fact is that this holds also for some other saturants<sup>25</sup>. Since the asteroid material may be well saturated with hydrogen (and possibly with some other gases), its  $Q$ -factor may be much affected.

It may be good to perform experiments, both on carbonaceous and siliceous rocks, at low frequencies and temperatures, and with a variety of combinations of the possible saturants. These experiments should give us the values for both shear and bulk quality factors. The current lack of experimental data gives us no choice but to start with the value 3300 obtained by Tittman for thoroughly degassed basalts, and then to use formula (5-10). This will give us, at  $T = 150 K$  and  $\omega = 10^{-5} Hz$ :

$$Q_{(shear)}^{(basalt)} \approx 100 \tag{5-11}$$

This value of the shear  $Q$ -factor for granites and basalts differs from the one chosen in Burns and Safronov (1979) only by a factor of 3. For carbonateous materials  $Q$  must be surely much less than that of silicates, due to weaker chemical bonds. So for carbonaceous rocks, it is for sure that

$$Q^{(carb)} < 100 \text{ ,} \tag{5-12}$$

though this upper boundary is still too high.

<sup>22</sup>A comprehensive study of the effective tidal  $Q$ -factors of the planets was performed by Goldreich and Soter (1966)

<sup>23</sup>Brennan mentions the decrease of  $Q$  with humidity, but unfortunately does not explain how his specimens were dried.

<sup>24</sup>These data were obtained by Brennan for strain amplitudes within the linearity range. Our case is exactly of this sort since the typical strain in a tumbling body will be about  $\sigma/\mu \approx \rho\Omega^2 a^2/\mu$ . For the size  $a \approx 1.5 \times 10^4 m$  and frequency not exceeding  $10^{-4} Hz$ , this strain is less than  $10^{-6}$  which is a critical threshold for linearity.

<sup>25</sup>like, for example, ethanol (Clark et al. 1980)

Consider asteroid 4179 Toutatis. This is an S-type asteroid analogous to stony irons or ordinary chondrites, so the solid-rock value of  $\mu Q$  may be applicable to it:  $\mu Q \approx 1.5 \times 10^{13} \text{ dyne/cm}^2 = 1.5 \times 10^{12} \text{ Pa}$ . Its density may be roughly estimated as  $\rho = 2.5 \times 10^3 \text{ kg/m}^3$  (Scheeres et al. 1998). Just as in the case of (5-8), let us measure the time  $\Delta t$  in years, the revolution period  $T$  in hours ( $T_{(hours)} = 175$ ), the maximal half-radius  $a$  in kilometers ( $a_{(km)} = 2.2$ ), and  $\theta$  in angular degrees ( $|\Delta\theta^\circ| = 0.01$ ). Then (4-35) will yield:

$$\Delta t_{(years)} \approx 5.1 \times 10^{-2} \frac{T_{(hours)}^3}{a_{(km)}^2} = 5.6 \times 10^4 \text{ years} \quad (5-13)$$

Presently, the angular-velocity vector  $\mathbf{\Omega}$  of Toutatis is at the stage of precession about  $A$  (see Fig.1). However its motion does not obey the restriction  $\langle \cos^2 \theta \rangle < 1/7$  under which (4-35) works well. A laborious calculation based on equations (2.16) and (A4) from Efroimsky (2000) and on formulae (1), (2) and (11) from Scheeres et al (1998) shows that in the case of Toutatis  $\langle \cos^2 \theta \rangle \approx 2/7$ . Since the violation is not that bad, one may still use (5-13) as the zeroth approximation. Even if it is a two or three order of magnitude overestimate, we still see that the chances for experimental observation of Toutatis' relaxation are slim.

This does not mean, though, that one would not be able to observe asteroid relaxation at all. The relaxation rate is sensitive to the parameters of the body (size and density) and to its mechanical properties ( $\mu Q$ ), but the precession period is certainly the decisive factor. Suppose that some asteroid is loosely-connected ( $\mu Q = 5 \times 10^{12} \text{ dyne/cm}^2 = 5 \times 10^{11} \text{ Pa}$  and  $\rho = 2 \times 10^3 \text{ kg/m}^3$ ), has a maximal half-size 17 km, and is precessing with a period of 30 hours, and *is not too close to the separatrix*. Then an optical resolution of  $|\Delta\theta^\circ| = 0.01$  degrees will lead to the following time interval during which a  $0.01^\circ$  change of the precession-cone half-angle will be measurable:

$$\Delta t_{(years)} \approx 2.12 \times 10^{-2} \frac{T_{(hours)}^3}{a_{(km)}^2} = 2 \text{ years} \quad (5-14)$$

which looks most encouraging. In real life, though, it may be hard to observe precession relaxation of an asteroid, for one simple reason: too few of them are in the states when the relaxation rate is fast enough. Since the relaxation rate is much faster than believed previously, most excited rotators have already relaxed towards their principle states and are describing very narrow residual cones, too narrow to observe. The rare exceptions are asteroids caught in the near-separatrix "trap". These are mimicing the principal state.

### 5.3. Loosely-Connected Asteroids

Above we mentioned that the mechanical structure of the small bodies is still in question. At present, most astronomers lean toward the so-called rubble-pile hypothesis, in regard to both asteroids and comets. The hypothesis originated in mid-sixties (Öpik 1966) and became popular in the end of the past century (Burns 1975; Weidenschilling 1981; Asphaug & Benz



1994; Harris 1996; Asphaug & Benz 1996; Bottke & Melosh 1996a,b; Richardson, Bottke & Love 1998; Bottke 1998, Bottke, Richardson & Love 1998; Bottke, Richardson, Michel & Love 1999, Pravec & Harris 2000).

This hypothesis rests on several arguments the main of which is the following: the large fast-rotating asteroids are near the rotational breakup limit for aggregates with no tensile strength. This is a strong argument, and one would find difficulty to object to it. Still, we would object to two other arguments often used in support this hypothesis. One such dubious argument is the low density of asteroid 253 Mathilde (about  $1.2 \text{ g/cm}^3$ ). This low density (Veverka et al 1998, Yeomans et al 1998) may be either interpreted in terms of the rubble-pile hypothesis (Harris 1998), or be put down to Mathilde being perhaps mineralogically akin to low-density carbonaceous chondrites, or be explained by a very high porosity. However, in our opinion, the word "porous" is not necessarily a synonym to "rubble-pile", even though in the astronomical community they are often used as synonyms. In fact, a material may have high porosity and, at the same time, be rigid.

Another popular argument, that we would contest, is the one about crater shapes. Many colleagues believe that a rigid body would be shattered into smithereines by collisions; therefrom they infer that the asteroids must be soft, i.e., rubble. In our opinion, though, a highly porous but still consolidated material may stand very energetic collisions without being destroyed, if its porous structure damps the impact. It is know from the construction engineering that some materials, initially friable, become relatively rigid after being heated up (like, for example, asphalt). They remain porous and may be prone to creep, but they are, nevertheless, sufficiently rigid and well connected.

We would also mention that, in our opinion, the sharply-defined craters on the surfaces of some asteroids witness **against** the application of the rubble-pile hypothesis to asteroids.

For these reasons, we expressed in Efroimsky & Lazarian (2000) our conservative opinion on the subject: *at least some asteroids are well-connected, though we are uncertain whether this is true for all asteroids*. This opinion met a cold reaction from the community. However, it is supported by the recentmost findings. The monolithic nature of 433 Eros is the most important of these (Yeomans 2000). Other include 1998KY26 studied in 1999 by Steven Ostro and his team: from the radar and optical observations (Ostro et al 1999), the team inferred that this 30-meter-sized body, as well as several other objects, is monolithic<sup>26</sup>.

Still, despite our conservative attitude toward the rubble-pile hypothesis, we have to admit that the main argument used by its proponents (the absence of large fast rotators) remains valid, and the question why the large fast-spinning asteroids are near the rotational breakup limit for loose aggregates is still awaiting its answer.

---

<sup>26</sup>We should mention here Vesta as a reliable example of an asteroid being a solid body of a structure common for terrestrial planets: Hubble images of Vesta have revealed basaltic regions of solidified lava flows, as well as a deep impact basin exposing solidified mantle.

As explained in the preceding subsection, to register relaxation of a solid-rock monolith may take thousands of years. However, if the body is loosely connected, the inelastic dissipation in it will be several orders faster and, appropriately, its relaxation rate will be several orders higher.

#### 5.4. Application to Asteroid 433 Eros in Light of Recent Observations

As already mentioned above, asteroid 433 Eros is in a spin state that is either principal one or very close to it. This differs from the scenario studied in (Black et al 1999). According to that scenario, an almost prolate body would be spending most part of its history wobbling about the minimal-inertia axis. Such a scenario was suggested because the gap between the separatrices embracing pole C on Fig.1 is very narrow, for an almost prolate body, and therefore, a very weak tidal interaction or impact would push the asteroid’s angular velocity vector  $\Omega$  across the separatrix, away from pole C. This scenario becomes even more viable due to the ”lingering effect” described in subsection 2.2, i.e., due to the relative slowing down of the relaxation in the closest vicinity of the separatrix.

Nevertheless, this scenario has not been followed by Eros. This could have happened for one of the following reasons: either the dissipation rate in the asteroid is high enough to make Eros well relaxed after the recentmost disruption, or the asteroid simply has not experienced impacts or tidal interactions for hundreds of millions of years.

The latter option is very unlikely: currently Eros is at the stage of leaving the main belt; it comes inside the orbit of Mars and approaches that of the Earth. It is then probable that Eros during its recent history was disturbed by the tidal forces that drove it out of the principal spin state. Hence we are left with the former option, one that complies with our theory of precession relaxation. The fact that presently Eros is within less than 0.1 degree from its principal spin state means that the precession relaxation is a very fast process, much faster than believed previously<sup>27</sup>.

#### 5.5. Unresolved issues

Our approach to calculation of the relaxation rate is not without its disadvantages. Some of these are of mostly aesthetic nature, but at least one is quite alarming.

As was emphasised in Section 3, our theory is adiabatic, in that it assumes the presence of two different time scales or, stated differently, the superposition of two motions: slow and fast. Namely, we assumed that the relaxation rate is much slower than the body-frame-

---

<sup>27</sup>Note that the complete (or almost complete) relaxation of Eros cannot be put down to the low values of the quality factor of a rubble pile, because this time we are dealing with a rigid monolith (Yeomans et al. 2000).

related precession rate  $\omega$  (see formulae (3-1) and (3-2)). This enabled us to conveniently substitute the dissipation rate by its average over a precession cycle. The adiabatic assertion is not necessarily fulfilled when  $\omega$  itself becomes small. This happens, for example, when the dynamical oblateness of an oblate ( $I_3 > I_2 = I_1 \equiv I$ ) body is approaching zero:

$$(h - 1) \rightarrow 0 \quad , \quad h \equiv I_3/I \quad . \quad (5-15)$$

Since in the oblate case  $\omega$  is proportional to the oblateness (see (5.4)), it too will approach zero, making our adiabatic calculation inapplicable. This is the reason why one cannot and shouldn't compare our results, in the limit of  $(h - 1) \rightarrow 0$ , with the results obtained by Peale (1973) for an almost-spherical oblate body.

Another minor issue, that has a lot of mathematics in it but hardly bears any physical significance, is our polynomial approximation (4-13 - 4-16 , 4-36 - 4-42) to the stress tensor. As explained in Section 4, this approximation keeps the symmetry  $\sigma_{ij} = \sigma_{ji}$  and exactly satisfies (1-20) with (4-12) plugged in. The boundary conditions are fulfilled exactly for the diagonal components of the tensor and approximately for the off-diagonal elements. In the calculation of the relaxation rate, this approximation will result in some numerical factor, and it is highly improbable that this factor differs much from unity.

A more serious difficulty of our theory is that it cannot, without further refinement, give a reasonable estimate for the duration of the near-separatrix slowing-down mentioned in subsection 2.2. On the one hand, many (formally, infinitely many) overtones of the base frequency  $\omega_1$  come into play near the separatrix; on the other hand, the base frequency approaches zero. Thence, it will take some extra work to account for the dissipation associated with the stresses oscillating at  $\omega_1$  and with its lowest overtones. (The dissipation due to the stresses at these low frequency cannot be averaged over their periods.)

There exists, however, one more, primary difficulty of our theory. Even though our calculation predicts a much faster relaxation rate than believed previously, it still may fail to account for the observed relaxation which seems to be even faster than we expect. According to the results obtained by NEAR, the upper limit on non-principal axis rotation is better than 0.1 angular degree. How to interpret such a tough observational limit on Eros' residual precession-cone width? Our theory does predict very swift relaxation, but it also shows that the relaxation slows down near the separatrix and, especially, in the closest vicinity of points  $A$  and  $C$  on Fig.1. Having arrived to the close vicinity of pole  $C$ , the angular-velocity vector  $\Omega$  must exponentially slow down its further approach to  $C$ . For this reason, a body that is monolithic (so that its  $\mu Q$  is not too low) and whose motion is sometimes influenced by tidal or other interactions, must demonstrate to us at least some narrow residual precession cone. As already mentioned, for the past million or several millions of years Eros has been at the stage of leaving the main belt. It comes inside the Mars orbit and approaches the Earth. Most probably, Eros experienced a tidal interaction within the said period of its history. Nevertheless it is presently in or extremely close to its principal spin state. The absence of a visible residual precession indicates that our theory may still be incomplete. In

particular, our  $Q$ -factor-based empirical description of attenuation should become the fair target for criticisms, because it ignores several important physical effects.

One such effect is material fatigue. It shows itself whenever a rigid material is subject to repetitive load. In the case of a wobbling asteroid or comet, the stresses are tiny, but the amount of repetitive cycles, accumulated over years, is huge. At each cycle, the picture of emerging stresses is virtually the same. Moreover, beside the periodic stresses, there exists a constant component of stress. This may lead to creation of "weak points" in the material, points that eventually give birth to cracks or other defects. This may also lead to creep, even in very rigid materials. The creep will absorb some of the excessive energy associated with precession and will slightly alter the shape of the body. The alteration will be such that the spin state becomes closer to the one of minimal energy. It will be achieved through the slight change in the direction of the principal axes in the body. If this shape alteration is due to the emergence of a considerable crack or displacement, then the subsequent damping of precession will be performed by a finite step, not gradually.

Another potentially relevant phenomenon is the effect that a periodic forcing (such as the solar gravity gradient) would have on the evolution and relaxation of the precession dynamics. It is possible that this sort of forcing could influence the precessional dynamics of the body<sup>28</sup>.

## 6. APPLICATION TO WOBBLING COMETS

### 6.1. Excitation of the Nucleus' Rotation by Reactive Torques

According to the widely accepted Whipple's model, comet nuclei are conglomerates of ice and dust, also called "dirty snowballs" (Whipple 1951). TV-images of P/Halley and P/Borrelly nuclei, obtained by spacecraft *Vega-1,2*, *GIOTTO* and *DEEP SPACE-1*, respectively, allow us to suppose that, generally, cometary nuclei have irregular nonconvex shapes with typical sizes  $R_*$  within the range of 1 to 10 kilometers. Numerically generated images of comets P/Halley and P/Borelly are presented on Figure 2 and Figure 3. A typical comet rotates slower than most asteroids of a like size. Rotational periods of most comets lie within the interval from several hours to several days.

Solar radiation instigates matter sublimation from the comet-nuclei surfaces; this process is especially intensive at heliocentric distances  $r < 3$  AU. Sublimated volatiles ( $H_2O$ ,  $CO$ ,  $CO_2$ , ...) and emansipated dust form an expanding atmosphere called coma. As a result, an Earth-based observer will not only register periodic brightness variations of the comet (feature common to spinning comets and asteroids), but will also observe effects specific to comets solely. These will be the morphological features of the coma. As an obvious

---

<sup>28</sup>We are thankful to Daniel Scheeres who drew our attention to this effect.

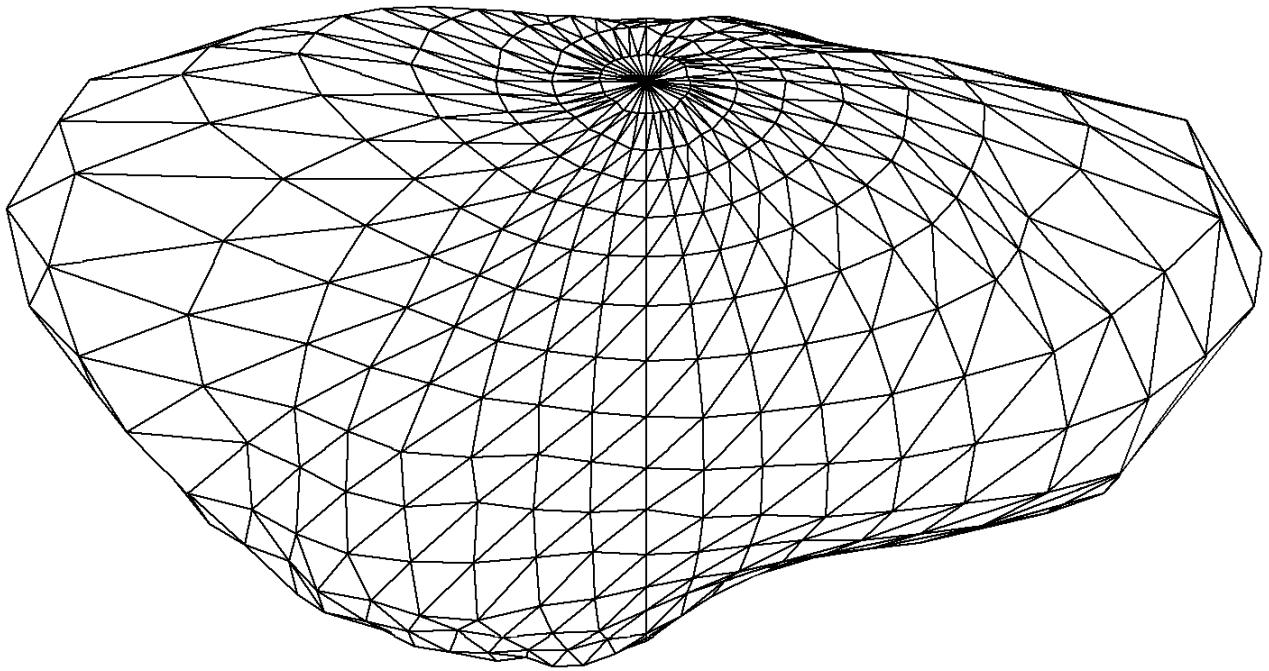


Fig. 2.— The general view of P/Halley nucleus, based on the numeric-shape model developed by Stooke and Abergel (1991) who used the Vega - 1, 2 and Giotto images.

example, we would mention the jets: lengthy narrow flows of matter, initiating on the nucleus' surface or close to it. A more subtle phenomenon will be twisting of such jets. As was pointed out by Whipple (Whipple 1951), evaporating matter should produce a reactive torque,  $\vec{\tau}$ , that acts on the nucleus and alters its spin state<sup>29</sup>. To calculate it, one can use formula

$$\vec{\tau} = - \sum_{j=1}^N Q_j (\vec{\mathbf{R}}_j \times \vec{\mathbf{v}}_j), \quad (6-1)$$

where  $N$  is the number of faces of the polyhedron approximating the nucleus' shape,  $Q_j$  is the rate of mass ejection by the  $j$ -th face,  $\vec{\mathbf{R}}_j$  is the radius vector of the face's centre in the body's principal frame of reference, and  $\vec{\mathbf{v}}_j$  is the effective velocity of the ejected matter. The process of mass ejection depends on local illumination conditions and on the current heliocentric distance. Its accurate description is a subject of a rather involved research (Crifo & Rodionov 1999). Various empirical models have been employed to study rotation evolution of cometary nuclei. For example, to model the relative dependence of the mass ejection rate on the heliocentric distance, the following expression was suggested in (Marsden, Sekanina & Yeomans 1973) and has been widely used since then:

$$g(r) = g_0 \left( \frac{r}{r_0} \right)^{-2.15} \left[ 1 + \left( \frac{r}{r_0} \right)^{5.093} \right]^{-4.6142}. \quad (6-2)$$

Here  $r_0 = 2.808$  AU,  $g_0$  is a normalising multiplier (whose its value can be chosen in such a way that  $g(q) = 1$ , where  $q$  stands for the perihelion distance).

In most publications on the topic, spin evolution of a comet nuclei due to reactive torques was studied through numeric integration of the equations of rotation (Wilhelm 1987, Julian 1990, Peale & Lissauer 1989, Samarasinha & Belton 1995, Jorda & Licandro 2002). A more systematic approach to the problem was developed in (Neishtadt, Scheeres, Sidorenko & Vasiliev 2002), where possible secular phenomena were studied by means of an accurate averaging procedure (Arnold 1978), and relevant physical parameters, that control the evolution of cometary rotation, were extracted.

Numeric and analytic investigations have revealed certain patterns in the spin evolution. For nuclei with fixed active regions, the direction of the angular momentum vector  $\vec{\mathbf{L}}$  typically spirals either toward the orbital direction of peak outgassing or opposite to it (Neishtadt, Scheeres, Sidorenko & Vasiliev 2002; Samarasinha & Belton 1995). The timescale  $t_R$  for the reactive torque to change the nucleus spin state can be estimated as

$$t_R \sim \frac{L_*}{(D_* R_*) Q_* V_* \Phi_*}, \quad (6-3)$$

---

<sup>29</sup>There are analogies between the spin-up of comets due to matter ejection and spin-up of grains due to ejection of H<sub>2</sub> atoms at the catalytic sites on grain surface. The theory of grain rotation due to such torques is discussed in Purcell (1979), Spitzer & McGlynn (1979), Lazarian & Draine (1997).

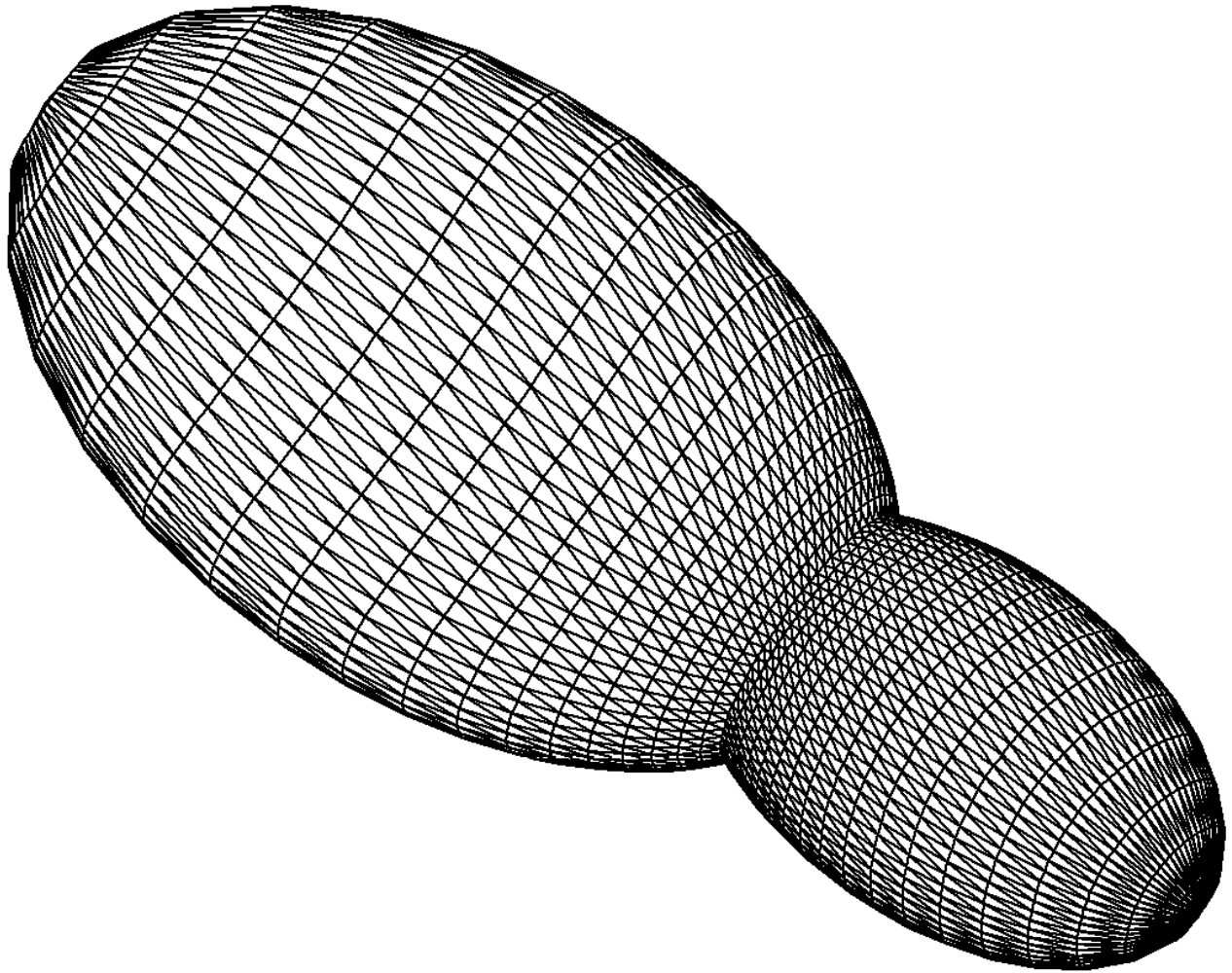


Fig. 3.— P/Borely nucleus: rough reconstruction based on Deep Space - 1 images. According to (Neishtadt, Scheeres, Sidorenko, Stooke & Vasiliev 2002), this nucleus can be approximated by a combination of two ellipsoids with major semiaxes  $1.6\text{ km}$ ,  $1.8\text{ km}$ ,  $3.0\text{ km}$ , and  $0.96\text{ km}$ ,  $1.08\text{ km}$ ,  $1.8\text{ km}$ , the distance between their centres being  $3.7\text{ km}$ .

$L_*$  being the nucleus angular momentum,  $Q_*$  being the total mass ejection rate at perihelion, and  $V_*$  being the effective exhaust velocity. The product  $(D_*R_*)$  can be interpreted as the torque’s arm. Here the dimensionless parameter  $D_*$  characterises the dependence of reactive torque on active zones’ distribution over the nucleus surface, while the dimensionless parameter  $\Phi_*$  is a certain integral characteristic of the nucleus’ heating on its orbit:

$$\Phi_* = \frac{1}{T} \int_0^T g(r(t))dt = \frac{(1 - e^2)^{3/2}}{\pi} \int_0^\pi \frac{g(r(\nu))d\nu}{(1 + e \cos \nu)^2}. \quad (6-4)$$

Here  $T$  and  $e$  are comet’s orbital period and eccentricity, while  $\nu$  is the nucleus true anomaly.

Although the long-term history of the nucleus spin state is dominated by reactive torques, we should not forget that nuclei are not perfectly rigid bodies. Splitting of comets’ nuclei by tidal stress, phenomenon that has been observed many a time by astronomers, has inspired some theoreticians to speculate that nuclei consist of weakly bonded components. This so-called “rubble-pile hypothesis” has been extended by some authors even to asteroids. As we already mentioned in one of the preceding sections of this review, this hypothesis has its *pro*’s and *con*’s and, therefore, both proponents and critics. What is certain thus far, is that at least some comets are indeed weak. For example, two unequal components of comet P/Borrelly are connected with an intermediate zone covered by a complicated network of cracks. This structure, well visible on the available images, has lead to a hypothesis that the P/Borrelly nucleus is assembled of two pieces in loose contact.

When the comet is not too far from the Sun, time  $t_R$  is, typically, much shorter than the internal-relaxation time. Nevertheless, it is possible that some qualitative properties of the nucleus’ rotation are associated with non-rigidity. In particular, since the timescale for wobble excitation by  $\vec{\tau}$  is often shorter than the damping time, it is reasonable to suppose that many cometary nuclei should be in excited rotational states after passing their perihelia (and sometimes even before approaching the perihelia). So far such an excited state has been reliably established for P/Halley only<sup>30</sup>. However, as we mentioned above there are several more comets whose spin state may be complex.

The small amount of tumbling comets observed thus far may be put down to one or both of the following reasons. The first is the still insufficient precision of our observation techniques. The second reason is the possibility of relaxation rate being much higher than believed previously.

---

<sup>30</sup>According to (Belton, Julian, Anderson & Mueller 1991), the long axis of P/Halley nucleus is inclined to the angular-momentum vector  $\vec{L}$  by  $\approx 66^\circ$  and is rotating about  $\vec{L}$  with a period of 3.69 days. The spin component about the long axis has a period of 7.1 days.



## 6.2. Parameters of the Comets

For the dirty ice Peale and Lissauer (1989) suggest, for Halley’s comet,  $\mu \approx 10^{10} \text{ dyne/cm}^2 = 10^9 \text{ Pa}$  while  $Q < 100$ . The latter number, 100, characterises attenuation in the solid ice. The question arises whether it is applicable to comets. In the preceding section we mentioned, in regard to asteroids, the “rubble-pile” hypothesis. Despite that hypothesis being fortified by various theoretical explanations, our attitude to it still remains conservative.

In the case of comets, though, this hypothesis may work. It is a well-established fact that comets sometimes get shattered by tidal forces. For example, Shoemaker-Levy 9 broke into 21 pieces on the perijove preceding the impact (Marsden 1993). In 1886 Comet Brooks 2 was rent into pieces by the jovian gravity (Sekanina 1982). Comet West disintegrated in 1976 (Melosh and Schenk 1993). It seems that *at least some comets are loosely consolidated aggregates, though we are unsure if this is the case for all comets*. Hopefully, our understanding of the subject will improve after the Deep Impact mission reaches its goal.

Loosely-connected comets, presumably, consist not so much of solid ice but more of firm (coarse-grained snow), material whose quality factor is of order unity. Hence the estimate

$$Q^{(comet)} \approx 1 \tag{6-5}$$

is, in our opinion, more realistic. So, let us assume  $\mu Q \approx 10^{10} \text{ dyne/cm}^2 = 10^9 \text{ Pa}$ . As for the average density of a comet, most probably it does not deviate much from  $1.5 \times 10^3 \text{ kg/m}^3$ . Indeed, on the one hand, the major part of the material may have density close to that of firm, but on the other hand a typical comet will carry a lot of crust and dust on and inside itself. Now, consider a comet of a maximal half-size 7.5 km (like that of Halley comet (Houppis and Gombosi 1986)) precessing with a period of 3.7 days  $\approx 89$  hours (just as Halley does<sup>31</sup>). If we once again assume the angular resolution of the spacecraft-based equipment to be  $|\Delta\theta^o| = 0.01$ , it will lead us to the following damping time:

$$\Delta t_{(years)} \approx 5.65 \times 10^{-5} \frac{T_{(hours)}^3}{a_{(km)}^2} = 0.7 \text{ year} \ . \tag{6-6}$$

This means that the cometary-relaxation damping may be measurable. It also follows from (6-6) that, to maintain the observed tumbling state of the Comet P/Halley, its jet activity should be sufficiently high.

## 6.3. Missions to Comets, and the Possible Nuclei-Dynamics Studies

One of the main results of our research is that, according to (6-6), wobble damping of comets may be registered within a one-year time span or so, provided the best available

---

<sup>31</sup>Belton et al 1991, Samarasinha and A’Hearn 1991, Peale 1992

spacecraft-based devices are used and the comet’s spin state is not too close to the separatrix. In the coming years a new generation of comet-aimed missions will increase the amount and quality of observations. Forthcoming enlargement of the comet database will result in deepening of our understanding of comet nuclei rotational dynamics.

The Stardust mission, that is to visit comet P/Wild 2, will be a fly-by one, and thus will not be able to trace the spin-state evolution. Spacecraft Deep Impact will approach comet 9P Tempel 1 on the 3 of July 2005, and will shoot a 500-kg impactor at 10 km/s speed, to blast a crater into the nucleus, to reveal its interior. Sadly, though, this encounter too will be short.

Rosetta orbiter is designed to approach 46/P Wirtanen and to escort it for about 2.5 years (Hubert & Schwehm 1991). Wirtanen seems to be a wobbling comet (Samarasinha, Mueller & Belton 1996), (Rickman & Jorda 1998), and one of the planned experiments is observation of its rotation state, to be carried out by the OSIRIS camera (Thomas et al 1998). The mission will start about 1.5 year before the perihelion, but the spin state will be observed only once, about a year before the perihelion, at a heliocentric distance of 3.5 AU. Three months later the comet should come within 3 AU which is to be a crucial threshold for its jetting activity: at this distance outgassing of water will begin. The strongest non-gravitational torques emerge while the comet is within this distance from the Sun. It is predominantly during this period that wobble is instigated. Hence, it may be good to expand the schedule of the spin-state observations: along with the measurement currently planned for 3.5 AU before perihelion, another measurement, at a similar heliocentric distance after the perihelion, would be useful. The comparison of these observations will provide information of the precession increase during the time spent by the comet within the close proximity to the Sun. Unfortunately, the Rosetta programme will be over soon afterwards, and a third observation at a larger distance will be impossible. The third observation performed well outside the 3 AU region might reveal the wobble-damping rate, and thereby provide valuable information about the composition and inner structure of the comet nucleus. It would be most desirable to perform such a three-step observation by the future escort missions to comets. What are the chances of success of such an experiment? On the one hand, the torques will not be fully eliminated after the comet leaves the 3 AU proximity of the Sun; though the outgassing of water will cease, some faint sublimation of more volatile species (like CO, CO<sub>2</sub>, CH<sub>3</sub>OH) will persist for long. On the other hand, the damping rate is high enough and a comparison of two observations separated by about a year will have a very good chance of registering wobble relaxation.

## 7. APPLICATION TO COSMIC-DUST ALIGNMENT

Inelastic relaxation is also important for cosmic-dust grains of sizes within the interval from  $3 \times 10^{-7}$  cm through  $10^{-4}$  cm. Such particles get their long axes aligned with respect to the interstellar magnetic field (see review by Lazarian 2000 for description of alignment

mechanisms). Absorption and emission of light by such particles is characterised by appropriate effective cross sections which depend upon the direction from which the observer looks at the particle. The difference between cross sections appropriate to the directions parallel to the long and short axes of the granule yields polarisation of the observed starlight, in case this light passes through clouds of aligned dust. Dust particles tend to align their orientation relative to the interstellar magnetic field, and it turns out that the polarisation of light depends upon the orientation and magnitude of the field. This circumstance gives birth to a very powerful technique for magnetic field studies, technique that rests on our understanding of the grain alignment, and on our ability to observe this alignment through measuring the polarisation of starlight passing through dust clouds.

Dust interact with the ambient media and rotate fast. There are a number of processes that allow grains to spin at a rate much larger than the typical rate of thermal rotation  $\omega_{th} \sim (kT_{gas}/J_{grain})^{1/2}$ , where  $J_{grain}$  is a typical angular momentum of the grain. For instance, formation of  $H_2$  molecules over catalytic sites on grain surface gives rise to the so-called Purcell rockets (Purcell 1979), which can spin up grains by ejecting nascent  $H_2$  molecules. Under such uncompensated torques the grain will spin-up to velocities much higher than  $\omega_{th}$ , and Purcell termed those velocities “suprathermal.”

It is obvious that grain wobble limits the degree to which the grain can be aligned. The ideas on the role of this wobble have been evolving through years. Initially it was assumed that the distribution of grain rotation among the axes is thermal  $I_i\omega_i^2 \sim kT_{grain}$  (see Jones & Spitzer 1967). Later Purcell (1979) realised that internal relaxation tends to bring grain angular momentum  $\vec{J}$  parallel to the axis of maximal inertia. He discussed both inelastic relaxation and a more subtle mechanism that he termed Barnett relaxation.

The Barnett effect is converse of the Einstein-Haas effect. The Einstein-Haas effect is rotation acquired by a paramagnetic body subject to remagnetisation. This happens because the flipping electrons transfer the angular momentum (associated with their spins) to the lattice. In the case of Barnett effect, the rotating body shares a part of its angular momentum with the electron subsystem; this sharing entails magnetisation. A typical value of the Barnett-induced magnetic moment is  $M \approx 10^{-19}\omega_{(5)} \text{ erg gauss}^{-1}$  (where  $\omega_{(5)} \equiv \omega/10^5\text{s}^{-1}$ ). Purcell offered the following illustrative explanation of the phenomenon. If a rotating body contains equal amount of spin-up and spin-down unpaired electrons, its magnetisation is nil. Its kinetic energy would decrease, with the total angular momentum remaining unaltered, if some share of the entire angular momentum could be transferred to the spins by turning some of the unpaired spins over (and, thus, by dissipating some energy). This potential possibility is brought to pass through the said coupling. Another way to understand the effect would be to recall that in the body frame of a free rotator the angular-momentum and angular-velocity vectors precess relative to the principal axes. Therefore, the Barnett magnetisation will, too, precess in the body frame. The resulting remagnetisation will be accompanied with energy dissipation (called paramagnetic relaxation).

An immediate outcome from granule magnetisation is the subsequent coupling of the

magnetic moment  $\mathbf{M}$  (directed along the grain angular velocity) with the interstellar magnetic field  $\mathbf{B}$ : the magnetic moment precesses about the magnetic line. What is important, is that this precession goes at an intermediate rate. On the one hand, it is slower than the grain’s spin about its instantaneous rotation axis. On the other hand, the precession period is much shorter than the typical time scale at which the relative-to- $\mathbf{B}$  alignment gets established<sup>32</sup>. The latter was proven by Dolginov & Mytrofanov (1976), for magnetisation resulting from the Barnett effect, and by Martin (1971), for magnetisation resulting from the grain’s charge.

Paramagnetic relaxation of the body in the external interstellar magnetic field had long been thought as the cause of the grain alignment. The “Barnett equivalent magnetic field”, i.e. the equivalent external magnetic field that would cause the same magnetization of the grain material, is  $H_{BE} = 5.6 \times 10^{-3} \omega_{(5)} \text{ G}$ , which is much larger than the interstellar magnetic field. Therefore the Barnett relaxation takes place on time scale  $t_{Bar} \approx 4 \times 10^7 \omega_{(5)}^{-2}$ , i.e., essentially instantly compared to the time of paramagnetic alignment  $\sim 10^{11} \text{ s}$  that establishes in respect to the external magnetic field<sup>33</sup> Thus Purcell (1979) concluded that  $\vec{\mathbf{J}}$  should be parallel to the axis of the grain major inertia.

From the discussion above it looks that the precise time of internal dissipation is irrelevant, if the internal alignment takes place faster than the alignment in respect to magnetic field. This is not true, however. Spitzer & McGlynn (1979), henceforth SM79 observed that adsorption of heavy elements on a grain should result in the resurfacing phenomenon that, e.g. should remove early sites of  $\text{H}_2$  formation and create new ones. As the result,  $\text{H}_2$  torques will occasionally change their direction and spin the grain down. SM79 showed that in the absence of random torques the spinning down grain will flip over preserving the direction of its original angular momentum. However, in the presence of random torques this direction will be altered with the maximal deviation inflicted over a short period of time just before and after the flip, i.e. during the time when the value of grain angular momentum is minimal. The actual value of angular momentum during this critical period depends on the ability of  $\vec{\mathbf{J}}$  to deviate from the axis of maximal inertia. SM79 observed that as the internal relaxation couples  $\vec{\mathbf{J}}$  with the axis of maximal inertia, it makes randomisation of grains during crossover nearly complete. Due to finite times of the internal relaxation the coupling is not complete and the grains preserve partially their alignment during crossovers. Calculations in SP79 showed that the Barnett relaxation is fast enough to make randomisation of grains nearly complete.

Lazarian & Draine (1997), henceforth LD97, revisited the problem of crossovers and

---

<sup>32</sup>A more exact statement is that the period of precession (about  $\mathbf{B}$ ) of the magnetic moment  $\mathbf{M}$  (and of  $Z$  aligned therewith) is much shorter than the mean time between two sequent flip-overs of a spinning granule (Purcell 1979, Roberge et al 1993)

<sup>33</sup>Radiative torques (Draine & Weingartner 1996, 1997) are currently favoured by observations as the mechanism of grain alignment (see Lazarian 2002). The alignment time for the radiative-torque mechanism is much larger than the internal dissipation time.

found out that the result is different if the thermal fluctuations associated with the relaxation mechanism are accounted for (see Lazarian & Roberge 1997). LD97 observed that the thermal fluctuations partially decouple  $\vec{J}$  and the axis of maximal inertia and therefore the value of angular momentum at the moment of a flip is substantially larger than SM79 assumed. Thus the randomisation during a crossover is reduced and LD97 obtained a nearly perfect alignment for interstellar grains rotating suprathermally, provided that the grains were larger than a certain critical size  $a_c$ . The latter size was found by equating the time of the crossover and the time of the internal dissipation  $t_{dis}$ . For  $a < a_c$  Lazarian & Draine (1999a) found new physical effects, which they termed “thermal flipping” and “thermal trapping”. The thermal flipping takes place as the time of the crossover becomes larger than  $t_{dis}$ . In this situation thermal fluctuations will enable flipovers. However, being random, thermal fluctuations are likely to produce not a single flipover, but multiple ones. As the grain flips back and forth, the regular (e.g.  $H_2$ ) torques average out and the grain can spend a lot of time rotating with thermal velocity, i.e. being “thermally trapped”. The paramagnetic alignment of grains rotating with thermal velocities is small (see above), and therefore grains with  $a < a_c$  are expected to be aligned only marginally. The picture of preferential alignment of large grains, as we know, corresponds to the Serkowski law and therefore the real issue is to find the value of  $a_c$ . In fact, Lazarian & Draine (1997) showed that  $a_c \sim 10^{-5}$  cm for the Barnett relaxation mechanism.

These finding stimulated more interest to the competing mechanism of internal energy dissipation, namely, to the inelastic relaxation of energy. Lazarian & Efroimsky (1999) redid the analysis of Purcell (1979) and obtained the expression for the relaxation time

$$t_i \approx a^{5.5} [1 + (c/a)^2]^4 \left(\frac{c}{a}\right)^{3/2} (\beta kT_{\text{gas}})^{-3/2} \mu Q \rho^{1/2} \frac{2^{11} 3^{-2.5}}{63(c/a)^4 + 20} \quad (7-1)$$

where the grain is modelled by a  $2a \times 2c \times 2c$  prizm ( $a < c$ ). Unlike our earlier expression (4-22), the kinetic energy of a rotating body is expressed using the factor of suprathermality, i.e. as  $\beta kT_{\text{gas}}$ . For crossovers thermal rotational velocities are important and for those Lazarian & Efroimsky concluded that inelastic relaxation may be dominant for grains larger than  $10^{-5}$  cm, provided that the grains are substantially flat (e.g. axes ratio is 4:1). The inelastic relaxation should also dominate atomic-size grains for which paramagnetic response fails (see discussion of paramagnetic relaxation within such grains in Lazarian & Draine 2000). As far as the critical-size value  $a_c$  was concerned, the study by Lazarian & Efroimsky (1999) did not change its appreciably apart from the case of extremely oblate grains.

However, in a recent paper, Lazarian & Draine (1999b) reported a new solid state effect that they termed “nuclear relaxation”. This is an analog of Barnett relaxation effect that deals with nuclei. Similarly to unpaired electrons nuclei tend to get oriented in a rotating body. However the nuclear analog of “Barnett equivalent” magnetic field is much larger and Lazarian & Draine (1999) concluded that the nuclear relaxation can be a million times faster than the Barnett relaxation. If this is true  $a_c$  becomes of the order  $10^{-4}$  cm, which

means that the majority of interstellar grains undergo constant flipping and rotate essentially thermally in spite of the presence of uncompensated Purcell torques. For particles rotating at a thermal Brownian rate, nuclear relaxation dominates the inelastic one for chunks up to 2 m. However, such large pieces rotate at a nonthermal rate and therefore inelastic relaxation rate that scales as  $\omega^3$  compared with  $\omega^2$  for the Barnett and nuclear relaxations is dominant.

The scaling of inelastic relaxation with angular velocity ensures that this mechanism is dominant for fast rotating dust particles. Such a rotation is possible due to differential scattering of left and right hand polarized photons (Dolginov & Mytrophanov 1976, Draine & Weingartner 1996, 1997). This difference in scattering cross sections arises naturally for irregular grains (Draine & Weingartner 1996). Unlike the H<sub>2</sub> torques proposed by Purcell (1979), the radiative torques are not fixed in the body coordinates. Therefore they do not average out during fast thermal flipping of the grain. Hence, it is likely that they can provide means for suprathreshold rotation for grains that are larger than the wavelength of the incoming radiation. The rate of internal relaxation for suprathresholdly rotating grains is important for special circumstances when the alignment happens very fast, e.g. in the stellar winds and comet atmospheres.

Another interesting consequence of the coupling of rotational and vibrational degrees of freedom, resulting from the inelastic dissipation, is the expected relation between microwave and infrared polarisation arising from ultrasmall ( $a < 10^{-7}$ ) grains. Dipole emission from those grains was invoked by Draine & Lazarian (1998a,b) to explain the anomalous microwave emission of galactic origin within the range of 10-90 GHz. This emission was shown to interfere with the intended measurements of Cosmic Microwave Background (CMB), and therefore attracted a lot of attention (see Lazarian & Prunet 2002 for a review). In view of the attempts to measure the CMB polarisation, it is important to know whether or not the emission from small grains will be polarised. This problem has not had been fully resolved as yet.

It is well known that the infrared emission from ultrasmall granules (the one of wavelength 12  $\mu$ m) takes place as the dust particles absorb UV photons. Can we check the alignment of ultrasmall grains via infrared polarimetry? The answer to this question depends on the efficiency of internal relaxation. Indeed, UV photons raise the grain temperature and randomise grain axes in relation to its angular momentum vector (see Lazarian & Roberge 1997) on the time scale of rotation-vibrational coupling. This is the time of internal relaxation. Taking the necessary figures for Barnett relaxation from Lazarian & Draine (1999), we get the randomisation time of a  $10^{-7}$  cm-sized grain to be  $2 \times 10^{-6}$  s, which is less than the grain cooling time. As a result, the emanating infrared radiation would be polarised very marginally. If, however, the Barnett relaxation is suppressed due to small-size effects (Lazarian & Draine 2000), the randomisation time is determined by inelastic relaxation and is  $\sim 0.1$  s, which would entail a partial polarisation of the infrared emission<sup>34</sup>. The uncer-

---

<sup>34</sup> We would remind, that even though the inelastic relaxation of a dust granule is several orders more

tainty of this estimate arises from extrapolation of dust properties and a classical treatment of an essentially quantum system. Further research in this direction is necessary.

## 8. CONCLUSIONS

1. In the article this far we have described the present situation in the studies of the dynamics of an unsupported top, and some of its applications to tumbling asteroids and comets and to the cosmic-dust particles. We addressed relaxation of excited (out of principal state) rotators through energy dissipation resulting from nutation-caused stresses.

2. In many spin states of an unsupported rotator, dissipation at frequencies different from the nutation frequency makes a major input into the inelastic-relaxation process. These frequencies are overtones of some "basic" frequency, that is LOWER than the precession frequency. This is a very unusual example of nonlinearity: the principal frequency (precession rate) gives birth not only to higher frequencies but also to lower frequencies.

3. In many spin states, the inelastic relaxation far more effective than believed hitherto.

4. However, if the rotation states that are close to the separatrix on Fig.2, the lingering effect takes place: both precession and precession-damping processes slow down. Such states (especially those close to the homoclinic point) may mimic the principal rotation state.

5. A finite resolution of radar-generated images puts a limit on our ability of recognising whether an object is nutating or not. Nutation-caused changes of the precession-cone half-angle may be observed. Our estimates show that we may be very close to observation of the relaxational dynamics of wobbling small Solar System bodies, dynamics that may say a lot about their structure and composition and also about their recent histories of impacts and tidal interactions. Monitoring of a wobbling comet during about a year after it leaves the 3 AU zone will, most probably, enable us to register its precession relaxation.

6. Measurements of the damping rate will provide us with valuable information on attenuation in small bodies, as well as on their recent histories of impacts and tidal interactions

7. Since inelastic relaxation is far more effective than presumed earlier, the number of asteroids expected to wobble with a recognisable half-angle of the precession cone must be lower than expected. (We mean the predictions suggested in (Harris 1994).) Besides, some of the small bodies may be in the near-separatrix states: due to the afore mentioned lingering effect, these rotators may be "pretending" to be in a simple rotation state.

8. Though the presently available theory predicts a much higher relaxation rate than believed previously, this high rate may still be not high enough to match the experimentally

---

effective that was presumed in (Purcell 1979), its intensity (as compared to the Barnett relaxation) depends upon the granule size (Lazarian & Efroimsky 1999). For the smallest granules, the Barnett dissipation still dominates (Lazarian & Draine 2000).

available data. In the closest vicinity of the principal spin state the relaxation rate must decrease and the rotator must demonstrate the "exponentially-slow finish". Asteroid 433 Eros is a consolidated rotator whose  $Q$ -factor should not be too low. It is possible that this asteroid was disturbed sometimes in its recent history by the tidal forces. Nevertheless, it shows no visible residual precession. Hence, there may be a possibility that we shall have to seek even more effective mechanisms of relaxation. One such mechanism may be creep-caused deformation leading to a subsequent change of the position of the principal axes in the body.

9. Inelastic coupling of the cosmic-dust grain's rotational and vibrational degrees of freedom influences randomisation of grain axes when an ultrasmall grain absorbs a UV photon. As a result, the microwave dipole emission arising from ultrasmall grains may be polarised, while the near-infrared emission arising from the same grains may be unpolarised.

## Acknowledgements

The authors wish to express their gratitude to the colleagues who participated, through direct collaboration as well as through advice and discussion, in the afore described research. ME would like to deeply thank William Newman for numerous fruitful discussions and for offering several highly illustrative examples that were included in the text. AL has the pleasure to thank Bruce Draine, Roger Hildebrand and John Mathis for stimulating exchanges. VS wants to acknowledge the contribution from Anatoly Neishtadt, Daniel Scheeres and Alexey Vasiliev. The work of AL was supported by the NSF through grant AST-0125544. The work of VS was supported through the NASA JURRISS Grant NAG5-8715 and INTAS Grant 00-221.



## REFERENCES

- Abramovitz, M., & I.A. Stegun 1965, *Handbook of Mathematical Functions, Chapter 16*, National Bureau of Standards
- Ahrens, T.J. 1995 Ed., *Mineral Physics & Crystallography. A Handbook of Physical Constants*. American Geophysical Union, Washington DC
- Arnold, V.I.: *Mathematical Methods of Classical Mechanics*. Springer, New York, 1978.
- Asphaug, E., S.J. Ostro, R. Hudson, D.J. Scheeres, & W. Benz. 1998, *Nature*, Vol. **393**, pp. 437
- Asphaug, E., & Scheeres, D.J. 1999, Deconstructing Castalia: Evaluating a Postimpact State. *Icarus*, Vol. **139**, pp. 383 - 386
- Asphaug, E., & W. Benz 1994. Density of comet Shoemaker-Levy 9 deduced by modelling breakup of the parent "rubble pile". *Nature*, Vol. **370**, pp. 120 - 124
- Asphaug, E., & W. Benz 1996. Size, density, and structure of comet Shoemaker-Levy 9 inferred from the physics of tidal breakup. *Icarus*, Vol. **121**, pp. 225 - 248
- Belton, M.J.S., B.E.A.Mueller, W.H. Julian, & A.J. Anderson. 1991. The spin state and homogeneity of Comet Halley's nucleus. *Icarus*, Vol. **93**, pp. 183 - 193
- Black, G.J, P.D.Nicholson, W.Bottke, J.Burns, & Allan W. Harris 1999. On a possible rotation state of (433) Eros. *Icarus*, Vol. **140**, pp. 239 - 242
- Bottke Jr., W.F., & Jay Melosh 1996a. Formation of asteroid satellites and doublet craters by planetary tidal forces. *Nature*, Vol. **381**, pp. 51 - 53
- Bottke Jr., W.F., & Jay Melosh 1996b. Binary Asteroids and the Formation of Doublet Craters. *Icarus*, Vol.**124**, pp. 372 - 391
- Bottke Jr., W.F., D.C.Richardson, P.Michel, & S.G.Love 1999. 1620 Geographos and 433 Eros: shaped by planetary tides? *The Astronomical Journal*, Vol. **117**, pp. 1921 - 1928
- Bottke Jr., W.F., D.C.Richardson, & S.Love 1998. *Planetary and Space Sciences*, Vol. **46**, pp. 311 - 322
- Bottke Jr., W.F. 1998. Are Asteroids Rubble Piles? *Paper for the 23rd Meeting of the International Seminars on Planetary Emergencies. Erice, Italy, 10 September 1998*. See also <http://astrosun.tn.cornell.edu/staff/bottke/rubble/rub.html>
- Brennan, B.J. 1981, in: Anelasticity in the Earth (F.D.Stacey, M.S.Paterson and A.Nicolas, Editors), Geodynamics Series 4, AGU, Washington.

- Burns, J. & V.Safronov 1973, Asteroid Nutation Angles. *MNRAS*, Vol. **165**, p. 403 - 411
- Burns, J. 1975, The Angular Momenta of Solar System Bodies: Implications for Asteroid Strengths. *Icarus*, Vol. **25**, p. 545 - 554
- Burns, J. 1977, in: *Planetary Satellites* (J.Burns, Ed.), Univ. of Arizona Press, Tuscon
- Burns, J. 1986, in: *Satellites* (J.Burns, Ed.), Univ. of Arizona Press, Tuscon
- Chernous'ko, F. 1968 Motion of a Rigid Body with Cavities Containing Viscous Liquid (in Russian)
- Clark V.A., B.R.Tittman & T.W.Spencer 1980. *J. Geophys. Res.*, Vol. **85**, p. 5190
- Crifo, J.F., & A.V.Rodionov: 1999, 'Modelling the circumnuclear coma of comets: objectives, methods and recent results', *Planetary and Space Science*, Vol. **47**, pp. 797–826.
- dell'Oro, A., P. Paolicchi, A. Cellino, V. Zappala, P. Tanga, & P. Michel. 2001. The Role of Families in Determining Collision Probability in the Asteroid Main Belt. *Icarus*, Vol. **153**, pp. 52 - 60.
- Denisov, G.G., & Novikov, V.V. 1987. Free motions of an elastic ellipsoid. *Izvestija AN SSSR. Mekhanika Tverdogo Tela*, Vol. **22**, No 6, pp. 69 - 74
- Dolginov, A. Z., & I. G.Mitrofanov. 1976. Orientation of Cosmic-Dust Grains. *Astrophysics and Space Science*, Vol. **43**, pp. 291 - 317
- Draine, B.T. & J.C. Weingartner. 1996. Radiative Torques on Interstellar Grains. I. Suprathermal Spin-up. *The Astrophysical Journal*, Vol. **470**, pp. 551-565
- Draine, B.T. & J.C. Weingartner. 1997. Radiative Torques on Interstellar Grains. I. Grain Alignment. *The Astrophysical Journal*, Vol. **480**, pp. 633 - 646
- Efroimsky, Michael 2002. Euler, Jacobi, and Missions to Comets and Asteroids. *Advances in Space Research*, Vol. **29**, pp. 725 - 734
- Efroimsky, Michael 2001. Relaxation of Wobbling Asteroids and Comets. Theoretical Problems. Perspectives of Experimental Observation. *Planetary & Space Science*, Vol. **49**, pp. 937 - 955
- Efroimsky, Michael, & A.Lazarian 2000. Inelastic Dissipation in Wobbling Asteroids and Comets. *Monthly Notices of the Royal Astronomical Society of London*, Vol. **311**, pp. 269 - 278
- Efroimsky, Michael 2000. Precession of a Freely Rotating Rigid Body. Inelastic Relaxation in the Vicinity of Poles. *Journal of Mathematical Physics*, Vol.**41**, p. 1854

- Euler, Leonhard 1765. *Theoria motus corporum solidorum seu rigidorum ex primis nostrae cognitionis principiis stabilita et ad omnes motus qui in huiusmodi corpora cadere possunt accomodata*. (In Latin). Recent edition: *Leonhard Euler. Series II. Opera mechanica et astronomica*. Vol. 3-4. Birkhauser Verlag AG, Switzerland 1999
- Fowles, G. & G. Cassiday 1986 *Analytical Mechanics*. Harcourt Brace & Co, Orlando FL
- Giblin, Ian, & Paolo Farinella 1997. Tumbling Fragments from Experiments Simulating Asteroidal Catastrophic Disruption. *Icarus*, Vol. **127**, pp. 424 - 430
- Giblin, Ian, G.Martelli, P.Farinella, P.Paolicchi, & M. Di Martino 1998. The Properties of Fragments from Catastrophic Disruption Events *Icarus*, Vol.**134**, pp. 77 - 112
- Goldreich, P., & S. Soter 1965. Q in the Solar System. *Icarus*, Vol. **5**, pp. 375 - 454
- Harris, Alan W. 1994. Tumbling Asteroids. *Icarus*, Vol. **107**, pp. 209 - 211
- Harris, Alan W. 1996. The rotational states of very small asteroids: evidence for "rubble-pile structure". *Lunar. Planet. Sci.*, Vol. **XXVII**, pp. 493 - 494
- Harris, Alan W. 1998. Making and Braking Asteroids. *Nature*, Vol. Vol. **393**, pp. 418 - 419
- Houppis, Harry L. F., & Gombosi, Tamas I. 1986. In: *Proc. 20-th ESLab Symp. on the Exploration of Halley's Comet, Vol. II*. European Space Agency, Paris.
- Hudson, R.S., & S. J. Ostro 1995. Shape and Non-Principal-Axis Spin State of Asteroid 4179 Toutatis. *Science*, Vol. **270**, pp. 84 - 86
- Hubert, M. C. E., & G. Schwehm 1991. *Space Science Review*, Vol. **56**, p. 109
- Jackson, Ian 1986, in: *Mineral and Rock Deformation. Laboratory Studies*, American Geophysical Union, Washington DC
- Jacobi, Karl Gustav Jacob 1829 *Fundamenta nova theoria functionum ellipticarum* Berlin
- Jacobi, Karl Gustav Jacob 1849, *Journal fur reine und angewandte Mathematik* (Berlin), Vol. **39**, pp. 293 - 350
- Jacobi, Karl Gustav Jacob 1882 *Gessamelte Werke*, Vol. **2**, pp. 427 - 510. Berlin
- Jewitt, D.: 1997, 'Cometary rotation: an overview', *Earth, Moon, and Planets*, Vol. **79**, pp. 35 - 53.
- Jones, R.V. & L. Spitzer. 1967. Magnetic Alignment of Interstellar Grains. *The Astrophysical Journal*, Vol. **147**, pp. 943 - 964
- Jorda, L., & J.Licandro. 2002. (*in press*), 'Modeling the rotation of comets', Proceedings of the IAU Colloquim 168, held in Nanjing, China. Pub. Astron. Soc. Pacific.

- Julian, W. 1990. The Comet Halley nucleus. Random jets. *Icarus*, Vol. **88**, pp. 355 - 371
- Karato, S.-i. 1998. *Pure and Applied Geophysics*, Vol. **153**, pp. 239
- Klinger J., A.-C. Levasseur-Regourd, N. Bouziani, & Enzian A. 1996. Towards a model of cometary nuclei for engineering studies for future space missions to comets. *Planet. Space. Sci.*, Vol. **44**, pp. 637 - 653
- Knopoff, L. 1963. Q. *Reviews of Geophysics*, Vol. **2**, pp. 625 - 629
- Lagrange, J. 1813 *Mecanique analytique*. Paris
- Lambeck, Kurt 1980 *The Earth's Variable Rotation: Geophysical Causes and Consequencies*, Cambridge University Press, Cambridge, U.K.
- Lambeck, Kurt 1988 *Geophysical Geodesy*, Oxford University Press, Oxford & NY
- Lamy, Philippe L., & Joseph A. Burns 1972. Geometrical Approach to a Torque-Free Motion of a Rigid Body Having Internal Energy Dissipation. *Amer. J. Phys.*, Vol. **40**, pp. 441 - 445
- Landau, L.D. & Lifshitz, E.M. 1976 *Mechanics*, Pergamon Press, NY
- Landau, L.D. & Lifshitz, E.M. 1970 *Theory of Elasticity*, Pergamon Press, NY
- Lazarian, A. 1994. Gold-Type Mechanisms of Grain Alignment. *MNRAS*, Vol. **268**, pp. 713 - 723
- Lazarian, A. 2000. Physics of Grain Alignment. In: *Cosmic Evolution and Galaxy Formation*, ASP Vol. **215**, pp. 69 - 79. Eds. Jose Franco, Elena Terlevich, Omar Lopez-Cruz. See also *astro-ph/0003314*
- Lazarian, A. & Draine, B.T. 1997. Disorientation of Suprathermally Rotating Grains and the Grain Alignment Problem. *The Astrophysical Journal*, Vol. **487**, pp. 248 - 258
- Lazarian, A. & Draine, B.T. 1999a. Thermal Flipping and Thermal Trapping: New Elements in Grain Dynamics. *The Astrophysical Journal*, Vol. **516**, pp. L37 - L40
- Lazarian, A. & Draine, B.T. 1999b. Nuclear Spin Relaxation within Interstellar Grains. *The Astrophysical Journal*, Vol. **520**, pp. L67 - L70
- Lazarian, A. & Draine, B.T. 2000. Resonance Relaxation. *The Astrophysical Journal*, Vol. **536**, pp. L15 - L18
- Lazarian, A. & Michael Efroimsky 1999. Inelastic Dissipation in a Freely Rotating Body: Application to Cosmic Dust Alignment. *MNRAS*, Vol. **303**, pp. 673 - 684

- Lazarian, A., & S. Prunet. 2002. Polarised Microwave Emission from Dust. In: *Proc. of the AIP Conference "Astrophysical Polarized Backgrounds,"* Eds.: S. Cecchini, S. Cortiglioni, R. Sault, and C. Sbarra, pp. 32 - 44
- Legendre, Adrien-Marie 1837 *Traite des fonctions elliptiques*
- Marsden, B. & S. Nakano 1993, IAU Circ. No 5800, 22 May 1993; Marsden, B. & A. Carusi 1993, IAU Circ. No 5801, 22 May 1993.
- Marsden, B.G., Z.Sekanina, & D.K.Yeomans. 1973. 'Comets and nongravitational forces.V', *Astron. J.*, Vol. **78**, pp. 211–225.
- Marsden, J. 2000. *Lectures on Mechanics*. Cambridge University Press.
- Martin, P.G. 1971. On interstellar grain alignment by a magnetic field. *Monthly Notices of the Royal Astronomical Society*, Vol. **153**, p. 279
- Meech, K. J., M. J. S. Belton, B. Mueller, M. Dicksion & H. Li 1993. Nucleus Properties of P/Schwassmann-Wachmann 1. *Astron. J.*, Vol. **106**, pp. 1222 - 1236.
- Melosh, H.J. & P. Schenk 1993. Split comets and the origin of crater chains on Ganymede and Callisto. *Nature*, Vol. **365**, pp. 731 - 733
- Miller, J.K., P.J. Antreasian, R.W. Gaskell, J. Giorgini, C.E. Helfrich, W.M Owen, B.G. Williams, & D.K. Yeomans, 1999, *Determination of Eros Physical Parameters for Near Earth Asteroid Rendezvous Orbit Phase Navigation*. Paper AAS 99-463, presented at the AAS/AIAA Astrodynamics Specialist Conference, Girdwood, Alaska, August 1999.
- Mitchell, J. W., D. L. Richardson. 2001. A Simplified Kinetic Element Formulation for the Rotation of a Perturbed Mass-Asymmetric Rigid Body. *Celestial Mechanics and Dynamical Astronomy*, Vol. **81**, pp. 13 - 25
- Molina, A., F. Moreno, & F. Martínez-López. 2002. Communication at the *ACM2002* International Conference. Berlin, 29 July - 2 August 2002.
- Muironen, K., & J.S.V. Lagerros. Inversion of shape statistics for small solar system bodies. *Astron. & Astrophys.* Vol. **333**, pp. 753 - 761 (1998)
- Neishtadt, A. I. 1980. *Mechanics of Solids*, Vol. **15**, No 6, pp. 21
- Neishtadt, A.I., D.J.Scheeres, V.V.Sidorenko, & A.A.Vasiliev: 2002, 'Evolution of comet nucleus rotation', *Icarus*, Vol. **157**, pp. 205–218.
- Nowick, A., & Berry, D. 1972 *Anelastic Relaxation in Crystalline Solids*, Acad. Press
- Okubo, S. 1982, *Geophys.J.*, Vol. 71, p. 647

- Ostro, S.J., R.F.Jurgens, K.D.Rosema, R.Winkler, D.Howard, R.Rose, D.K.Slade, D.K.Youmans, D.B.Cambell, P.Perillat, J.F.Chandler, I.I.Shapiro, R.S.Hudson, P.Palmer, & DePater, I. 1993. *BAAS*, Vol.**25**, p. 1126
- Ostro, S.J., R.S.Hudson, R.F.Jurgens, K.D.Rosema, R.Winkler, D.Howard, R.Rose, M.A.Slade, D.K.Yeomans, J.D.Giorgini, D.B.Campbell, P.Perillat, J.F.Chandler, & I.I.Shapiro, 1995. Radar Images of Asteroid 4179 Toutatis. *Science*, Vol. **270**, pp. 80 - 83
- Ostro, S.J., R.S.Hudson, K.D.Rosema, J.D.Giorgini, R.F.Jurgens, D.Yeomans, P.W.Chodas, R.Winkler, R.Rose, D.Choate, R.A.Cormier, D.Kelley, R.Littlefair, L.A.Benner, M.L.Thomas, & M.A.Slade 1999. Asteroid 4179 Toutatis: 1996 Radar Observations. *Icarus*, Vol. **137**, pp. 122-139
- Ostro, S.J., P.Pravec, L.A.Benner, R.S.Hudson, L.Sarounova, M.Hicks, D.L.Rabinovitz, J.V.Scotti, D.J.Tholen, M.Wolf, R.F.Jurgens, M.L.Thomas, J.D.Giorgini, P.W.Chodas, D.Yeomans, R.Rose, R.Frye, K.D.Rosema, R.Winkler, & M.A.Slade 1999. Radar and Optical Observations of Asteroid 1998 KY26. *Science*, Vol. **285**, pp. 557 - 559
- Peale, S. J. 1973. Rotation of Solid Bodies in the Solar System. *Rev. Geophys. Space Phys.*, Vol. **11**, pp. 767 - 793
- Peale, S.J., & J.J.Lissauer, 1989. Rotation of Halley's Comet. *Icarus*, Vol. **79**, pp. 396-430
- Peale, S.J. 1992. On LAMs and SAMs for the rotation of Halley's Comet. In: *Asteroids, Comets, Meteors 1991*. A.Harris and E. Bowles Eds. Lunar and Planetary Institute, Houston TX, pp. 459 - 467.
- Peale, S.J., P.Cassen & R.T.Reynolds 1979. Meltin of Io by tidal dissipation. *Science*, Vol. **203**, pp. 892 - 894
- Poisson 1813 *J. Ecol. Polyt.*, Cah. 16, p. 274-264
- Pravec, P., & A. W. Harris 2000. Fast and Slow Rotation of Asteroids. *Icarus*, Vol. **148**, pp. 12 - 20
- Prialnik, D. 1999. Modelling gas and dust release from comet Hale-Bopp. *Earth, Moon and Planets*, Vol. **77**, pp. 223 - 230
- Prendergast, Kevin H. 1958. The Effects of Imperfect Elasticity in Problems of Celestial Mechanics. *Astronomical Journal*, Vol. **63**, pp. 412- 414
- Prokof'eva, V.V., L.G.Karachkina, & V.P.Tarashchuk 1997. Light Variations of Asteroid 1620 Geographos during its Encounter with the Earth in 1994. *Astronomy Letters*, Vol. **23**, pp. 758 - 767.

- Prokof'eva, V.V., V.P.Tarashchuk, & L.G.Karachkina. 1996. Precession of asteroid 1620 Geographos. *Odessa Astronomical Publications*, Vol. **9**, p. 188.
- Purcell, E.M. 1979. Suprathermal Rotation of Interstellar Grains. *Astrophysical Journal*, Vol. **231**, p. 404 - 416
- Richardson, D.L., & J.W. Mitchell. 1999. A Simplified Variation of Parameters Approach to Euler's Equations. *Journal of Applied Mechanics*, Vol. **66**, pp. 273 - 276
- Richardson, D.C., W.F.Bottke, & S.G.Love 1998. Tidal Distortion and Disruption of Earth-Crossing Asteroids. *Icarus*, Vol. **134**, pp. 47 - 76
- Rickman, H., & L. Jorda 1998. Comet 46P/Wirtanen, The Target of the Rosetta Mission, *Adv. Space Res.*, Vol. **21**, pp. 1491 - 1504
- Ryabova, G.O. 2002. Asteroid 1620 Geographos: Rotation. *Solar System Research*. Vol. **36**, pp. 168 - 174
- Roberge, W.G., T. A. DeGraff, & J.E. Flaherty. 1993. The Langevin Equation and Its Application to Grain Alignment in Molecular Clouds *Astrophys. J.*, **418**, p. 287
- Ryan, M.P., & J.Y.K.Blevins. 1987 U.S. Geological Survey Bulletin, Vol.1764, p.1
- Sagdeev R.Z., Szego K., Smith B.A., Larson S., Merenyi E., Kondor A., & Toth I. 1989, The rotation of P/Halley. *Astron.J.*, Vol. **97**, pp. 546 - 551
- Samarasinha, N.H., & M.F. A'Hearn 1991, Observational and dynamical constraints on the rotation of Comet P/Halley. *Icarus*, Vol. **93**, pp. 194 - 225
- Samarasinha, N.H., B.E.A. Mueller, & M.J.S. Belton. 1996, Comments on the Rotational State and Non-gravitational Forces of Comet 46P/Wirtanen. *Planetary and Space Science*, Vol. **44**, pp. 275 - 281
- Samarasinha, N.H., & M.J.S. Belton 1995, Long-term evolution of rotational stress and nongravitational effects for Halley-like cometary nuclei. *Icarus*, Vol. **116**, pp. 340 - 358
- Samarasinha, N.H., B. Mueller & M. Belton 1999. *Earth, Moon and Planets*, Vol. **77**, p. 189
- Scheeres, D.J., S.J.Ostro, R.S.Hudson, S.Suzuki, & E. de Jong 1998. Dynamics of Orbits Close to Asteroid 4179 Toutatis. *Icarus*, Vol. **132**, pp. 53-79
- Sekanina Z. 1982, in: *Comets* (L.Wilkening, Ed.) U. of Arizona Press, Tuscon, pp. 251 - 287
- Stacey, Frank D. 1992. *Physics of the Earth*, Brookfield Press, Brisbane
- Stooke, P. J., & A. Abergel. 1991. Morphology of the Nucleus of Comet P/Halley *Astronomy & Astrophysics*, Vol. **248**, pp. 656 - 668

- Spitzer, L., Jr. & T.A. McGlynn. 1979. Disorientation of Interstellar Grains in Suprathermal Rotation. *The Astrophysical Journal*. Vol. **231**, pp. 417 - 424
- Synge, J.L., & B. Griffith 1959. *Principles of Mechanics, Chapter 14*, McGraw-Hill NY
- Thomas, N., and 41 colleagues, 1998. *Advances in Space Research*, Vol. **21**, pp. 1505
- Thomson, W.T. 1961 *Introduction to Space Dynamics*. Wiley, NY
- Tittman, B., L.Ahlberg, & J.Curnow 1976, in *Proc. 7-th Lunar Sci. Conf.*, pp. 3123 - 3132
- Tschoegl, N.W. 1989. *The Phenomenological Theory of Linear Viscoelastic Behaviour. An Introduction*. Springer-Verlag, NY
- Vasil'ev, V.G., & V.M.Kovtunenکو. 1969. On stability of revolution of a spacecraft with hinge-joined rods. *Kosmicheskie Issledovanija*, Vol. **7**, No 5. (*in Russian*)
- Veverka, J., P.Thomas, A.Harch, B.Clark, J.F.Bell III, B.Carcich, J.Joseph, C.Chapman, W.Merline, M.Robinson, M.Malin, L.A.McFadden, S.Murchie, S.E.Hawkins III, R.Farquhar, N.Izenberg, & A.Cheng 1997. NEAR's Flyby of 253 Mathilde. Images of the Asteroid. *Science*, Vol. **278**, pp. 2109 - 2114
- Weidenschilling, S. 1981. How fast can an asteroid spin? *Icarus*, Vol. **46**, pp. 124 - 126
- Whipple, F.L.: 1951, 'A comet model.I. Acceleration of comet Encke' *Astrophys. J.*, Vol. **113**, pp. 464–474.
- Wilhelm, Klaus. 1987. Rotation and precession of comet Halley. *Nature*, Vol. **327**, pp. 27 - 30
- Yoder, C.F. 1982. Tidal Rigidity of Phobos. *Icarus*, Vol. **49**, pp. 327 - 346
- Yeomans, D.K., J.-P.Barriot, D.W.Dunham, R.W.Farquhar, J.D.Gorgini, C.E.Helfrich, A.S.Konopliv, J.V.McAdams, J.K.Miller, W.M.Owen Jr, D.J.Scheeres, S.P.Synnott, & B.G.Williams. 1997. Estimating the Mass of Asteroid 253 Mathilde from Tracking Data During the NEAR Flyby. *Science*, Vol. **278**, pp. 2106 - 2108
- Yeomans, D.K., P.G.Antreasian, J.-P.Barriot, S.R.Chesley, D.W.Dunham, R.W.Farquhar, J.D.Giorgini, C.E.Helfrich, A.S.Konopliv, J.V.McAdams, J.K.Miller, W.M.Owen Jr., D.J.Scheeres, P.C.Thomas, J.Veverka, & B.G.Williams. 2000. Radio Science Results During the NEAR-Schoemaker Spacecraft Rendezvous with Eros. *Science*, Vol. **289**, pp. 2085 - 2088